A Paleogene extensional arc flare-up in Iran

Charles Verdel,[1,2] Brian P. Wernicke,[1] Jamshid Hassanzadeh,[1] and Bernard Guest[3]

Received 8 October 2010; revised 16 February 2011; accepted 2 March 2011; published 22 June 2011.

[1] Arc volcanism across Iran is dominated by a Paleogene pulse, despite protracted and presumably continuous subduction along the northern margin of the Neotethyan ocean for most of Mesozoic and Cenozoic time. New U-Pb and $^{40}Ar/^{39}Ar$ data from volcanic arcs in central and northern Iran constrain the duration of the pulse to ~17 Myr, roughly 10% of the total duration of arc magmatism. Late Paleocene-Eocene volcanic rocks erupted during this flare-up have major and trace element characteristics that are typical of continental arc magmatism, whereas the chemical composition of limited Oligocene basalts in the Urumieh-Dokhtar belt and the Alborz Mountains which were erupted after the flare-up ended are more consistent with derivation from the asthenosphere. Together with the recent recognition of Eocene metamorphic core complexes in central and east central Iran, stratigraphic evidence of Eocene subsidence, and descriptions of Paleogene normal faulting, these geochemical and geochronological data suggest that the late Paleocene-Eocene magmatic flare-up was extension related. We propose a tectonic model that attributes the flare-up to decompression melting of lithospheric mantle hydrated by slab-derived fluids, followed by Oligocene upwelling and melting of enriched mantle that was less extensively modified by hydrous fluids. We suggest that Paleogene magmatism and extension was driven by an episode of slab retreat or slab rollback following a Cretaceous period of flat slab subduction, analogous to the Laramide and post-Laramide evolution of the western United States.

Citation: Verdel, C., B. P. Wernicke, J. Hassanzadeh, and B. Guest (2011), A Paleogene extensional arc flare-up in Iran, *Tectonics*, *30*, TC3008, doi:10.1029/2010TC002809.

1. Introduction

[2] Flux-melting models of arc volcanism predict that magma production is closely related to the supply of slab-derived hydrous fluids [e.g., *Gill*, 1981; *McCulloch and Gamble*, 1991; *Davies and Stevenson*, 1992]. Regardless of whether these fluids originate from subducted sediments [e.g., *Plank and Langmuir*, 1993] or hydrous melts of oceanic crust [e.g., *Elliott*, 2004], the rate at which they are replenished is closely tied to subduction rate [e.g., *Davies and Bickle*, 1991]. Although subduction rate and volcanic output are correlated in some cases [*Huang and Lundstrom*, 2007], it has become increasingly clear that magma production in some arcs is distinctly episodic. Relatively short magmatic pulses that seem to be uncorrelated with subduction rate, and which account for a disproportionately large fraction of the total magmatic production of an arc, have been referred to as "flare-ups" [*Ducea*, 2001; *Ducea and Barton*, 2007]. The existence of flare-ups suggests that simple flux-melting models may not fully account for magma generation processes that operate at some convergent margins. One of these processes could be mantle upwelling, which is linked with volcanism in back-arc basins [e.g., *Gribble et al.*, 1998] and may generate melting beneath volcanic arcs as well [e.g., *Sisson and Bronto*, 1998].

[3] Two notable examples of magmatic flare-ups in the geological record include (1) the Sierra Nevada batholith of western North America, where despite a >100 My history of subduction, magmatism was dominated by two pulses, each lasting only 10–20 Myr [*Ducea*, 2001; *Van Buer and Miller*, 2010], and (2) episodic Miocene to Recent mafic volcanism in the Andean Puna Plateau [e.g., *Kay et al.*, 2005]. In both of these examples geologic evidence of synmagmatic compression has led to models that link flare-ups to shortening of the overriding tectonic plate. In the model of *Kay and Kay* [1993], shortening and thickening induce phase changes that increase the density of the base of the crust, eventually leading to delamination of both lower crust and lithospheric mantle. Partial melting of rising asthenospheric mantle subsequently generates a magmatic pulse. *Ducea and Barton* [2007] presented isotopic evidence that the Sierra Nevada arc flare-up was induced by lithospheric thickening, with a large fraction of the magma derived from melting of the lower crust.

[4] Magmatic flare-ups also occur in extensional settings. Perhaps the best known example is the mid-Tertiary

[1]Division of Geological and Planetary Sciences, California Institute of Technology, Pasadena, California, USA.
[2]Now at Department of Geology, University of Kansas, Lawrence, Kansas, USA.
[3]Department of Geoscience, University of Calgary, Calgary, Alberta, Canada.

0278-7407/11/2010TC002809

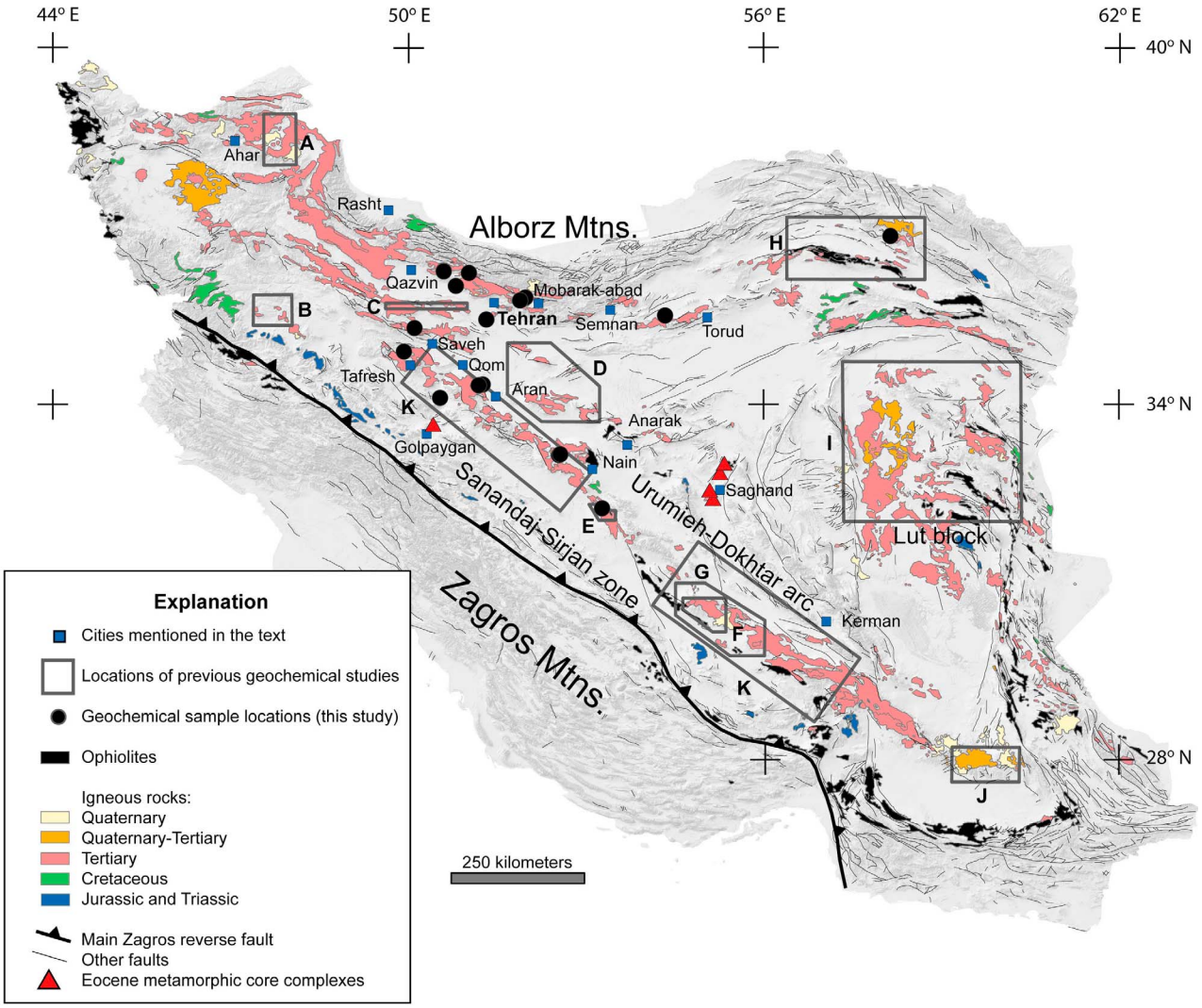

Figure 1. Map of Iran highlighting Cenozoic and Mesozoic igneous rocks (modified from *Haghipour and Aghanabati* [1985] and *Pollastro et al.* [1999]). Eocene metamorphic core complexes from *Moritz et al.* [2006] and *Verdel et al.* [2007]. Previous geochemical studies: A, *Alberti et al.* [1979]; B, *Boccaletti et al.* [1976]; C, *Ghorbani* [2006]; D, *Amidi et al.* [1984]; E, *Amidi and Michel* [1985]; F, *Förster et al.* [1972]; G, *Hassanzadeh* [1993]; H, *Spies et al.* [1984]; I, *Jung et al.* [1984]; J, *Dupuy and Dostal* [1978]; K, *Omrani et al.* [2008].

"ignimbrite flare-up" in western North America [*Coney*, 1978]. Although the event occurred during subduction, a notable attribute of this flare-up is the broad distribution of magmatism inland from the Cretaceous arc, at distances of up to 1000 km from the plate boundary [e.g., *Noble*, 1972]. Volcanism during the flare-up was broadly coincident with the formation of metamorphic core complexes in the Basin and Range province [e.g., *Gans et al.*, 1989; *Wernicke*, 1992] and may have been related to mantle upwelling and sinking of the Farallon slab [*Humphreys*, 1995; *Humphreys et al.*, 2003].

[5] In this paper we address a magmatic flare-up similar to the mid-Tertiary event in the western United States that occurred during Paleogene time in Iran. Eocene calc-alkaline volcanic rocks blanket most of central Iran, the southern Alborz Mountains, and the northern Lut block (Figure 1). Reported thicknesses of Paleogene volcanic and sedimentary rocks are ~3–9 km in the Urumieh-Dokhtar belt (Figure 1) in central Iran and the Alborz Mountains in northern Iran [e.g., *Förster et al.*, 1972; *Annells et al.*, 1975; *Hassanzadeh*, 1993; *Morley et al.*, 2009]. The preservation of kilometer-scale thicknesses of volcanic strata over tens of thousands of square kilometers in both regions is unique in regard to the magmatic history of Iran. Indeed, the thicknesses of volcanic deposits and the implied volume of erupted material (probably of order 10^6 km^3) are rather extraordinary by global standards.

[6] Marine fossils within the Iranian arc stratigraphy indicate that volcanism was largely shallow marine and was dominated by an Eocene pulse [e.g., *Stöcklin*, 1968; *Berberian and King*, 1981]. Volcanism occurred while Neotethyan oceanic crust was being slowly subducted beneath Iran at a relatively constant rate of ~3 cm/yr [*McQuarrie et al.*, 2003], but magmatism before and after

the flare-up was minor to absent within both the Urumieh-Dokhtar belt and the Alborz Mountains, despite a history of subduction that may have begun as early as the Late Triassic, as discussed below.

[7] The cause of the Iranian flare-up and, in fact, Iranian Tertiary volcanism in general has been a matter of debate for some 30 years. The linear trend of the Urumieh-Dokhtar belt parallel to the Arabia-Eurasia suture (Figure 1), arc-like trace element characteristics of Eocene volcanism, and the steady northward motion of the northern Arabian margin from an initial position >1300 km south of the present-day suture [*McQuarrie et al.*, 2003], have led to the predominant view that the Urumieh-Dokhtar belt is a conventional continental arc analogous to the Andes [e.g., *Förster et al.*, 1972; *Dewey et al.*, 1973; *Berberian et al.*, 1982; *Sengör et al.*, 1993]. In contrast, *Amidi et al.* [1984] and *Amidi and Michel* [1985], on the basis of major element data from alkaline Tertiary volcanics, argued that the Urumieh-Dokhtar belt was a linear rift basin unrelated to subduction. These disparate viewpoints, rooted in a debate over the relative importance of subduction versus rifting in generating arc volcanism, are the most common explanations for Paleogene magmatism within Iran. Triggering of the flare-up has been attributed to opening of rifts or back-arc basins [*Amidi et al.*, 1984; *Amidi and Michel*, 1985; *Kazmin et al.*, 1986; *Vincent et al.*, 2005], flattening of subduction trajectory [*Berberian and Berberian*, 1981; *Shahabpour*, 2007], and changes in subduction rate [*Takin*, 1972; *Pazirandeh*, 1973; *Kazmin et al.*, 1986]. By comparison with the examples of North and South American flare-ups noted above, key issues that could aid in evaluating these hypotheses include (1) the age and duration of the flare-up; (2) the basic geochemical attributes of flare-up volcanism; (3) the regional tectonic regime (i.e., compressional or extensional) at the time of the flare-up; and (4) the spatial relationship between flare-up volcanism and older elements of the Iranian arc system. For example, because paleogeographic reconstructions of Arabia-Eurasia convergence have become increasingly detailed in recent years [*McQuarrie et al.*, 2003; *Agard et al.*, 2006, 2007], it may be possible to directly evaluate scenarios linking the flare-up with changes in convergence rate if the age of the flare-up is known with sufficient precision. As another example, the rifting hypothesis would seem to clearly predict an overall extensional regime during Eocene time, while explanations calling on shallowing of subduction angle to generate the flare-up [e.g., *Berberian and Berberian*, 1981] might be inferred to predict Eocene contraction.

[8] In this paper, we present new data bearing on the first two issues listed above, and offer new interpretations of longstanding geologic observations that bear on the latter two. We have obtained U-Pb and $^{40}Ar/^{39}Ar$ age constraints on volcanic rocks in the Alborz Mountains and Urumieh-Dokhtar magmatic belts, as well as major and trace element data from primitive mafic rocks erupted during and after the flare-up. We utilize these data and interpretations to formulate a proposed tectonic framework for the Cenozoic evolution of Iran and the Paleogene arc flare-up.

2. Regional Geology

[9] Summarized below are the events most pertinent for the generation of arc magmas across central Iran. More complete discussions of the tectonic and paleogeographic evolution of Iran can be found in the work by *Stöcklin* [1968], *Berberian and King* [1981], *Dercourt et al.* [1986], *Ramezani and Tucker* [2003], and *McQuarrie et al.* [2003].

[10] The substrate of the Iranian Paleogene arc magmas include various continental blocks believed to have been situated along the northern margin of Gondwana in late Paleozoic time, separated from Eurasia by the Paleotethys ocean. These blocks, which now occupy central and northern Iran, were rifted from Gondwana during Permian time, opening the Neotethys oceanic basin in their wake [e.g., *Ramezani and Tucker*, 2003; *Hassanzadeh et al.*, 2008], and leaving the Iranian fragments situated between one ocean basin that was expanding and another that was being consumed [*Berberian and King*, 1981]. A regional unconformity separating rocks as young as Middle Triassic from overlying strata as old as Rheatic-Liassic [*Stöcklin*, 1968] is generally interpreted as marking the Middle to Late Triassic closure of Paleotethys [e.g., *Horton et al.*, 2008; *Wilmsen et al.*, 2009]. Plutons of roughly the same age in the Sanandaj-Sirjan zone of southwest Iran (Figure 1) suggest that subduction of Neotethys beneath Iran initiated at about this time [*Berberian and Berberian*, 1981; *Berberian et al.*, 1982; *Dercourt et al.*, 1986; *Kazmin et al.*, 1986; *Arvin et al.*, 2007], and may, in fact, have been a direct consequence of the collision between northern Iran and Eurasia [*Berberian and King*, 1981]. Continued subduction and arc magmatism through the Mesozoic is indicated by scattered Jurassic to Cretaceous intrusive rocks, mainly within the Sanandaj-Sirjan zone (Figure 1) [*Berberian and Berberian*, 1981].

[11] Ophiolites near the Main Zagros reverse fault, separating the Sanandaj-Sirjan zone from the Zagros Mountains (Figure 1), are generally interpreted to mark the suture between Arabia and Eurasia [e.g., *Agard et al.*, 2005]. The timing of collision between Arabia and Eurasia is a matter of considerable controversy, however. Salient recent findings include paleogeographic reconstructions from *McQuarrie et al.* [2003] suggesting that collision occurred between 10 and 20 Ma. Thermochronology data from plutons in the Alborz Mountains reveal a period of rapid middle to late Miocene cooling that may reflect uplift of the Alborz Mountains in response to Arabia-Eurasia collision [*Axen et al.*, 2001; *Guest et al.*, 2006b]. Apatite (U-Th)/He cooling ages from the Saghand region of central Iran (Figure 1) are ~20 Ma and suggest an early Miocene period of N-S shortening [*Verdel et al.*, 2007]. In the northern segment of the suture zone, *Agard et al.* [2005] interpret 23–25 Ma flyschoid strata as overlapping the Main Zagros reverse fault, suggesting a minimum age for collision at this location. Identification of microfossils within widespread foreland basin fill in the Zagros Mountains (Bakhtiyari Formation) establish a late Oligocene-early Miocene age for these deposits, providing another minimum age constraint on the timing of collision [*Fakhari et al.*, 2008]. Furthermore, (U-Th)/He data from thrust sheets in the central Zagros Mountains indicate early Miocene exhumation [*Gavillot et al.*, 2010]. These lines of evidence all suggest late Oligocene-Miocene collision. Alternatively, a number of stratigraphic observations can be interpreted in terms of a late Eocene onset of contractile tectonics throughout the region (see review by *Allen and Armstrong* [2008]). For example, a Tertiary sedimentary and volcanic succession in the Talysh region of

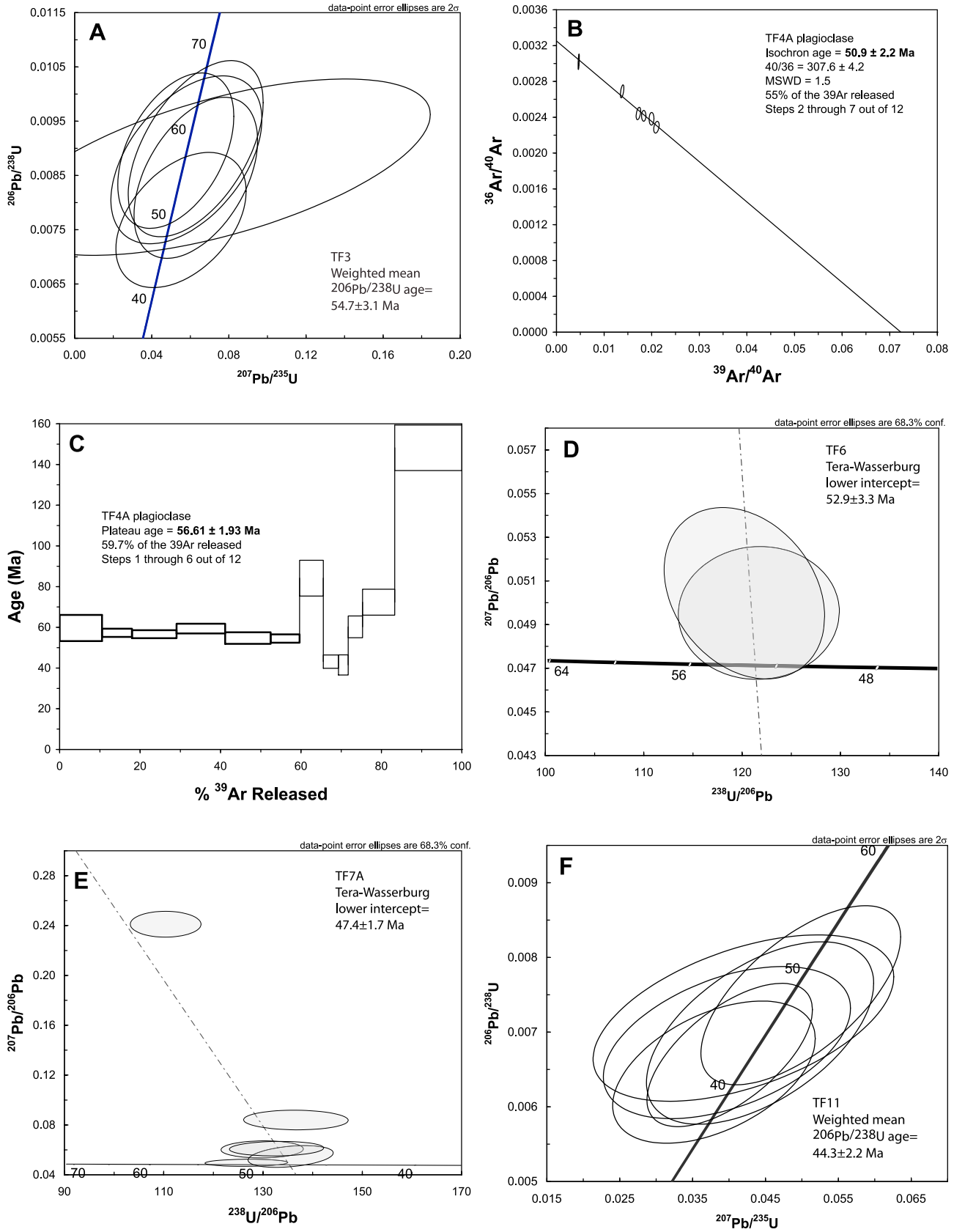

Figure 2. (a-k) U-Pb and $^{40}Ar/^{39}Ar$ geochronology data for volcanic rocks from the Alborz Mountains and the Urumieh-Dokhtar belt.

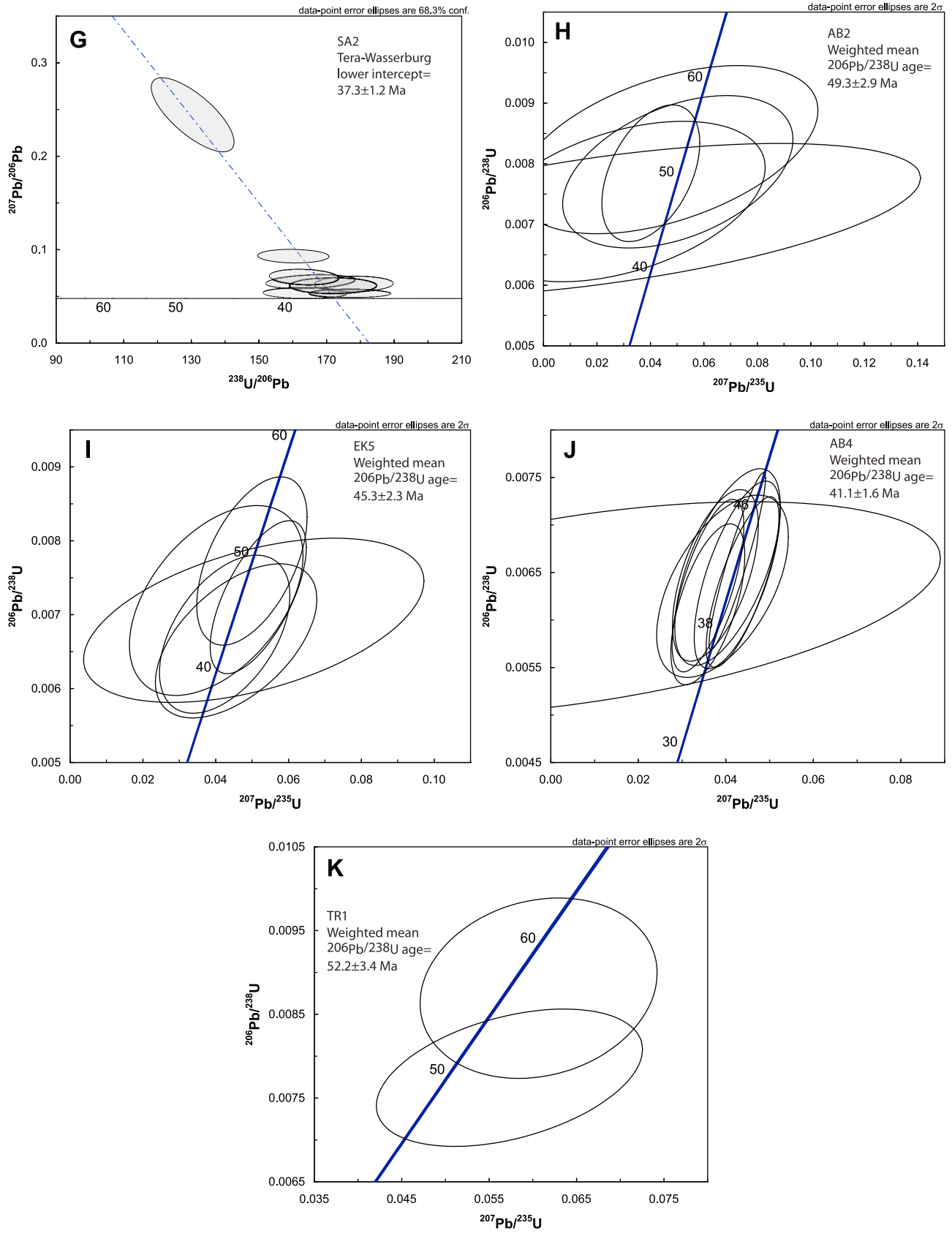

Figure 2. (continued)

Azerbaijan may record a late Eocene-early Oligocene transition from regional extension to compression [*Vincent et al.*, 2005]. Recognizing that contrasting interpretations exist as to the final timing of closure of Neotethys, our overall interpretation of Iranian regional geology is that subduction of Neotethys beneath Eurasia was ongoing from as early as Late Triassic until at least late Oligocene time, some 175 million years.

3. Paleogene Arc Stratigraphy

[12] Paleogene volcanic rocks crop out in three general regions within Iran (Figure 1). The first is along a NW-SE belt that extends ~1500 km across the central part of the country. This belt, named Urumieh-Dokhtar in reference to localities at either end, terminates rather abruptly to the southeast near the Pakistan border and merges with volcanic rocks in the Lesser Caucasus and Alborz Mountains to the northwest. The belt is subparallel to, and approximately 175–200 km northeast of, the Main Zagros reverse fault, although Neogene NE-SW shortening within the Sanandaj-Sirjan zone may have lessened this gap since the time of active subduction [*Berberian and Berberian*, 1981]. The Lesser Caucasus/Alborz belt extends southeast to near Semnan, where it becomes discontinuous and extends into eastern Iran. The third region is a large area of Tertiary volcanic rocks in the Lut block of eastern Iran [e.g., *Jung et al.*, 1984].

[13] Our study is focused on the Alborz Mountains and a portion of the Urumieh-Dokhtar belt near the longitude of Tehran. In this region, Tertiary volcanic rocks unconformably overlie a Mesozoic stratigraphy consisting primarily of marine carbonates and siliciclastic rocks. In general, Mesozoic volcanic strata beneath the Eocene basal conglomerate are thin or absent, although there are important exceptions. In particular, in the northern Alborz Mountains near Qazvin (Figure 1) there are locally up to 1.5 km of Upper Cretaceous (Senonian, circa 89–65 Ma) intermediate to mafic lavas [*Annells et al.*, 1975]. In a nearby area to the southeast, there are nearly 1000 m of similar rocks of mid-Cretaceous age (Aptian-Albian, circa 125–100 Ma).

[14] The Tertiary stratigraphic sequences in the Alborz Mountains and the NW Urumieh-Dokhtar belt are remarkably similar. In both areas, the older part of the Tertiary section includes volcanic rocks of wide-ranging composition interbedded with marine and continental sedimentary strata. Evidence of submarine volcanism has been widely reported [*Stöcklin*, 1968; *Förster et al.*, 1972; *Alberti et al.*, 1979; *Amidi et al.*, 1984; *Spies et al.*, 1984; *Amidi and Michel*, 1985; *Hassanzadeh*, 1993]. This part of the section, which makes up the majority of the Tertiary outcrop area shown in Figure 1, is typically overlain, in both arc segments, by the late Eocene-early Oligocene Lower Red Formation, consisting of conglomerate, sandstone, shale, and gypsum, as well as relatively limited pyroclastic deposits and volcanic flows. Conformably overlying the Lower Red Formation are ~1200 m of marine limestones and marls comprising the Oligocene to early Miocene Qom Formation [*Stöcklin and Setudehnia*, 1977; *Reuter et al.*, 2009]. Mafic lava flows are present within the Qom Formation in the Urumieh-Dokhtar belt and immediately below the Qom-correlative Gand Ab limestones in the western Alborz Mountains, where they have yielded a $^{40}Ar/^{39}Ar$ whole rock age of 33 Ma [*Guest et al.*, 2007b]. The Qom Formation is conformably overlain by gypsum-bearing red beds of the Miocene Upper Red Formation and continental Pliocene and Quaternary sediments.

4. Results

4.1. Geochronology

[15] Samples of Paleogene volcanic rocks and subvolcanic intrusions were collected from the Urumieh-Dokhtar belt and Alborz Mountains, mainly near the longitude of Tehran (Figure 1). Radiometric ages (U-Pb and $^{40}Ar/^{39}Ar$) were determined for 11 of these samples, all of which are from stratigraphic positions below the Lower Red Formation. U and Pb isotopic measurements of hand-picked zircon grains (Data Set S1) were made with the UCLA ims1270 ion probe using analytical methods described by *Grove et al.* [2003].[1] U-Pb data are plotted on concordia diagrams or Tera-Wasserburg diagrams (Figure 2). $^{40}Ar/^{39}Ar$ data from hand-selected plagioclase grains (Data Set S2) were measured at the Nevada Isotope Geochronology Lab using the same basic procedures as outlined by *Verdel et al.* [2007]. These data are plotted as conventional Ar release spectra and inverse isochrons (Figure 2). Latitude and longitude coordinates for geochronology samples are in Data Set S3.

4.1.1. Urumieh-Dokhtar U-Pb and $^{40}Ar/^{39}Ar$ Geochronology

[16] North of the town of Tafresh in central Iran, ~200 km southwest of Tehran, a cross section through the Urumieh-Dokhtar belt is exposed in the relatively undeformed limb of a NW-SE trending syncline. In this area, complexly faulted Mesozoic carbonates and siliciclastic strata are unconformably overlain by the typical arc sequence described above: Paleocene-Eocene volcanic and sedimentary rocks, the Lower Red Formation, carbonates and mafic volcanics of the Qom Formation, and the Upper Red Formation (Figure 3). We collected a transect of silicic to intermediate volcanic samples that extends from the base through the middle part of the volcanic section.

[17] Zircons from an andesite flow near the base of the volcanic section have a U-Pb age of 54.7 ± 3.1 Ma (2σ) (Figures 2a and 3). A green tuff bed slightly higher in the section has a plagioclase $^{40}Ar/^{39}Ar$ isochron age of 50.9 ± 4.4 Ma (2σ) (Figure 2b) and a plateau age of 56.6 ± 3.9 Ma (2σ) (Figure 2c), both of which are statistically indistinguishable from the U-Pb age of the underlying andesite. We consider 54.7 ± 3.1 Ma to be our best estimate for the age of the oldest Tertiary arc volcanism preserved along the transect. Ages decrease up section (Figures 2d and 2e) and reach 44.3 ± 2.2 Ma (Figure 2f) in the middle of the volcanic section (Figure 3). We collected an additional sample of welded tuff from near the top of the volcanic section ~60 km northwest of Saveh (Figure 1). Zircons from this tuff have a U-Pb age of 37.3 ± 1.2 Ma (Figure 2g).

4.1.2. Alborz Mountains U-Pb and $^{40}Ar/^{39}Ar$ Geochronology

[18] The Eocene Karaj Formation in the Alborz Mountains of northern Iran is comprised of 3000–4000 m of

[1] Auxiliary materials are available at ftp://ftp.agu.org/apend/tc/2010tc002809.

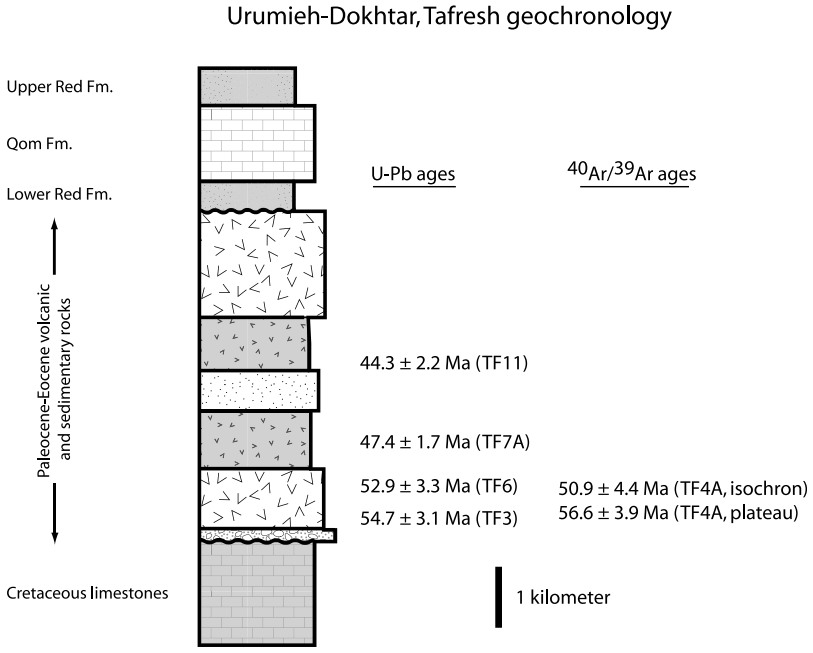

Figure 3. Composite stratigraphy of Cretaceous through Miocene volcanic and sedimentary rocks in the Tafresh area (modified from *Emami* [1991]) showing general stratigraphic position of geochronology samples. Thicknesses are approximate. Sample numbers in parentheses.

volcanic, volcaniclastic, and sedimentary strata that have been subdivided into the following members: Lower Shale, Middle Tuff, Asara Shale, Upper Tuff, and Kandavan Shale [e.g., *Annells et al.*, 1975; *Stöcklin and Setudehnia*, 1977]. We collected samples of tuffaceous rocks from within the Karaj Formation along the Chalus Road north of Tehran (Figures 1 and 4). We determined U-Pb zircon ages of 49.3 ± 2.9 Ma for the Middle Tuff (Figure 2h), 45.3 ± 2.3 Ma for a tuff within the Asara Shale (Figure 2i), and 41.1 ± 1.6 Ma for the Upper Tuff (Figure 2j).

[19] In addition, we collected a sample of rhyolitic tuff from the lower part of the Eocene volcanic section ~80 km west of Torud in the eastern Alborz Mountains (Figure 1) [*Alavi and Hushmandzādeh*, 1976]. Zircons from this tuff yield an average U-Pb age of 52.2 ± 3.4 Ma (Figure 2k). Finally, an $^{40}Ar/^{39}Ar$ age of 37.2 ± 0.38 Ma was determined from biotites in gabbros that intrude the Karaj Formation ENE of Tehran near Mobarak-abad (Figure 1).

4.2. Geochemistry

4.2.1. Previous Work

[20] In comparison with many other arcs, modern, high-quality geochemical investigations of Iranian Tertiary volcanism have been limited. We compiled approximately 300 major element analyses from 11 previous studies focused on the Iranian arcs (see Figure 1 for the locations of these prior studies). These data were compared with large data sets from the Andes and Cascades that seem to typify the basic geochemical attributes of continental arc magmatism. First-order compositional differences between volcanism in Iran and these well-characterized arcs are evident by comparing each region on total alkali-silica (TAS) diagrams (Figure 5). Previous studies have noted that Iranian Tertiary volcanism seems to have been significantly more alkaline than arc magmatism in the more extensively studied regions [e.g., *Amidi et al.*, 1984; *Kazmin et al.*, 1986; *Aftabi and Atapour*, 2000]. Although potentially an important clue that Iranian Tertiary volcanism differed in some way from well-characterized examples of continental arcs, a rigorous analysis of the older Iranian data is difficult because many of the analyses lack trace element, petrographic, and stratigraphic information. We discuss below a new suite of samples that, although limited in number, are from key stratigraphic intervals within the Tertiary arcs and capture much of the compositional diversity that has been established by previous studies.

4.2.2. Major Element Classification of New Samples

[21] Twenty-one new samples of mafic to intermediate lavas and subvolcanic intrusions were collected in the Alborz Mountains near Tehran, and in the Urumieh-Dokhtar belt, primarily between the cities of Saveh and Nain (Figures 1 and 5a–5e). Mafic samples were preferentially collected in order to minimize the potential effects of crustal contamination and fractional crystallization. Major element oxide and trace element compositions of these 21 samples were determined using X-ray fluorescence (XRF) at the Ronald B. Gilmore XRF laboratory at the University of Massachusetts (Tables 1 and 2). Details of the analytical procedure can be found in the work by *Rhodes* [1996].

[22] The samples range from 44 to 59 wt % SiO_2. On a TAS diagram (Figure 5e), 18 of the 21 samples plot within the field defined by the data sets from the Andes and Cascades, and the remainder (samples TA5, NA3, and TRD5) are more alkaline. These highly alkaline samples, all of which contain the zeolite mineral analcime ($NaAlSi_2O_6 \cdot H_2O$), would conventionally be called shoshonites. The 18

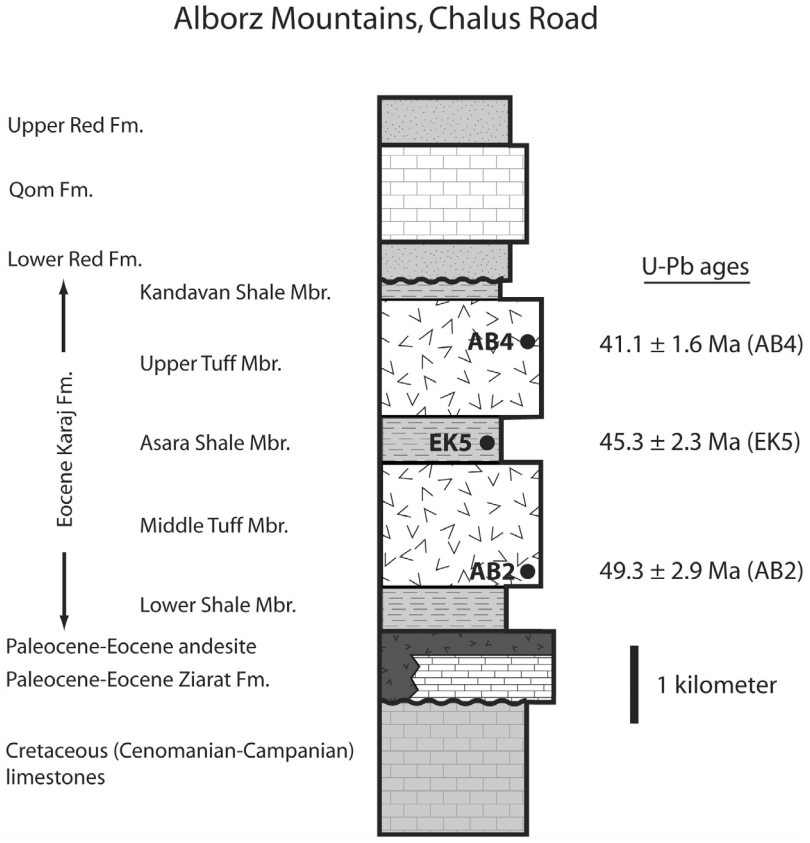

Figure 4. Cretaceous through Miocene stratigraphy of the Chalus Road area summarizing geochronological results (modified from *Haghipour et al.* [1987]). Thicknesses are approximate. Sample numbers in parentheses. Sample EK5 is a tuff within the Asara Shale Member.

remaining samples can be subdivided into two groups based on the SiO_2 content normally specified as the divide between basalts and andesites: five have >53 wt % SiO_2, and 13 have <53 wt % SiO_2. Of the basaltic andesite and andesite samples with >53 wt % SiO_2, four of them (AN3, DEHNAR1, QM2, and AN5) are classified as medium-K andesites using the scheme proposed by *Gill* [1981], and the other (AR3) is high K. Eight of the 13 samples with <53 wt % SiO_2 are basalts, and the remainder are basanites, trachybasalts, or basaltic trachyandesites. According to the definition of *Macdonald and Katsura* [1964], eight of these mafic samples are alkalic, three would be classified as "transitional" [*Sheth et al.*, 2002], and the remaining two are subalkalic.

4.2.3. Trace Element Data

[23] We plot our trace element data according to a threefold subdivision of the sample suite based on major elements, including (1) the five samples with >53 wt % silica ("andesites"; Figure 6a); (2) the five subalkaline and transitional basalts (Figure 6b); and (3) the eight alkaline basalts (Figure 6c). Of the five andesite samples, four of them (AN5, AR3, DEHNAR1, and QM2) are Eocene and exhibit strong depletions in Nb (Figure 6a). The other (AN3) is an Oligocene dike that has small positive spikes for the LILEs Ba, K, and Sr, but essentially no depletions of the HFSE. The subalkaline and transitional basalts, all of which are Eocene, have relatively uniform trace element compositions (Figure 6b). These basalts are depleted in the HFSE Nb, Zr, Ti, and Y and have positive spikes for the LILE Ba, K, and Sr. Of the eight alkaline basalts (Figure 6c), three are Eocene and five are Oligocene. Two Eocene samples within this group (TA1 and TA3) have prominent negative Nb spikes.

5. Discussion

5.1. Duration of the Flare-up

[24] Based on the oldest and youngest U-Pb ages from the main period of volcanism, which are corroborated by $^{40}Ar/^{39}Ar$ ages, we estimate that the magmatic flare-up lasted from 54.7 ± 3.1 Ma (latest Paleocene-early Eocene) until 37.3 ± 1.2 Ma (late Eocene), implying a duration of 17.4 ± 1.7 Myr. It is quite conceivable that the duration and absolute age of the flare-up varies by location within Iran (for instance from north to south or east to west), or that the full duration of the flare-up is not preserved in some areas where the top or bottom of the Paleocene-Eocene sequence is an unconformity. Our data also do not constrain potential variations in magmatic productivity that may have occurred during the flare-up, although these variations appear substantial [*McQuarrie et al.*, 2003]. However, the similarity of our results from the Urumieh-Dokhtar belt with those from the Alborz Mountains suggests that ~55 to 37 Ma is an accurate estimate for the duration of the flare-up as a whole.

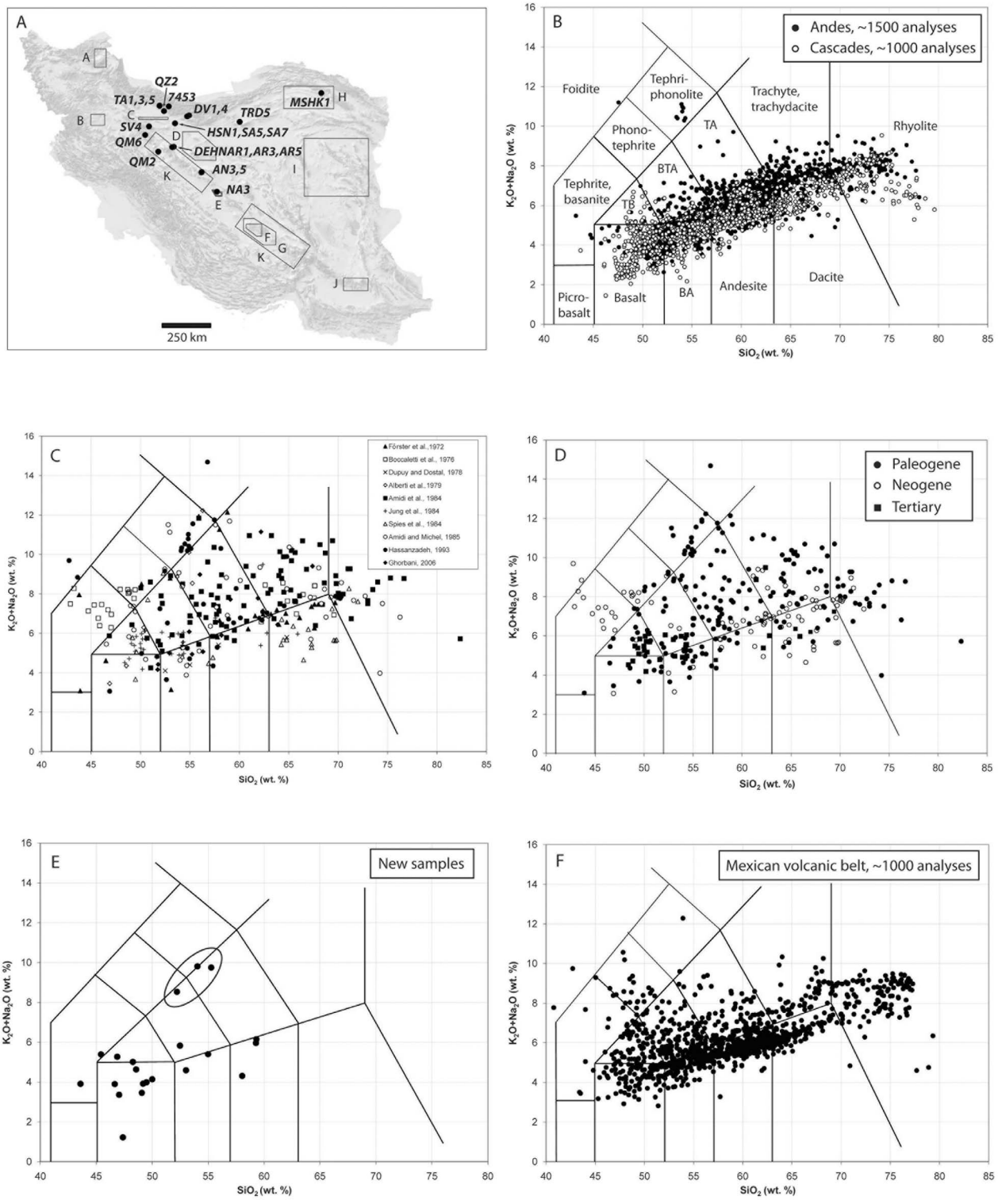

Figure 5. Total alkali-silica diagrams. (a) Sample locations and previous geochemical studies A-K as in Figure 1. (b) Data from ~1500 Andean samples and ~1000 Cascades samples, compiled from the GEOROC database. Nomenclature is also shown. Abbreviations: BA, basaltic andesite; BTA, basaltic trachyandesite; TA, trachyandesite; TB, trachybasalt. (c) Data from ~300 Iranian Tertiary samples, compiled from the sources shown in Figure 5a. (d) Same data as Figure 5c coded by age. (e) Twenty-one new Iranian Tertiary samples; oval drawn around shoshonitic samples. (f) Approximately 1100 samples from the Mexican volcanic belt, compiled from the GEOROC database.

Table 1. Major and Trace Element Compositions of Iranian Paleogene Basanites and Basalts

	Sample										
	7453	TA3	DV1	DV4	HSN1	MSHK1	QM6	QZ2	SA5	SA7	TA1
Latitude (WGS84)	36.20155	36.23063	35.78198	35.73080	35.40928	36.82298	34.87202	35.98157	36.22677	35.41140	36.24017
Longitude (WGS84)	51.00782	50.58340	51.95788	51.87353	51.30103	58.12228	49.90792	50.79127	50.58443	51.30395	50.58243
Lithology	Basanite	Basanite	Basalt	Basalt	Basalt	Basalt	Basalt	Basalt	Basalt	Basalt	Basalt
SiO_2 (%)	43.59	45.42	47.38	49.07	49.18	48.27	48.56	46.65	50.00	49.49	47.04
TiO_2 (%)	1.53	1.22	0.42	1.04	1.06	1.58	1.42	1.97	1.09	1.04	1.08
Al_2O_3 (%)	15.46	14.22	11.63	15.37	19.06	17.13	19.08	15.34	18.84	18.69	16.57
Fe_2O_3 (%)	10.74	12.23	10.15	9.94	10.10	9.56	11.41	12.75	10.12	10.13	10.46
MnO (%)	0.17	0.23	0.19	0.17	0.17	0.15	0.20	0.20	0.17	0.17	0.17
MgO (%)	8.48	7.29	15.98	9.85	5.30	8.02	4.29	8.31	4.95	5.78	8.95
CaO (%)	9.73	13.38	12.75	10.43	10.86	9.21	9.93	10.20	10.06	10.13	11.96
Na_2O (%)	2.62	4.03	0.85	1.76	2.68	4.08	3.98	3.25	2.80	2.71	2.76
K_2O (%)	1.29	1.36	0.37	1.70	1.24	0.93	0.65	0.65	1.34	1.28	0.60
P_2O_5 (%)	0.68	0.50	0.05	0.32	0.28	0.57	0.18	0.44	0.31	0.33	0.36
Total (%)	94.29	99.88	99.77	99.65	99.93	99.50	99.70	99.76	99.68	99.75	99.95
Nb (ppm)	27	12.7	1.0	4.9	6.6	23.0	8.6	14.5	7.0	6.0	3.5
Zr (ppm)	142	114	18	66	73	199	134	119	84	73	36
Y (ppm)	23	25.4	10.1	16.5	18.4	22.5	25.8	25.3	20.1	19.0	17.1
Sr (ppm)	775	1247	424	552	646	673	220	878	642	699	738
U (ppm)	0.69	0	0	0	0	0	0	0	0	0	0
Rb (ppm)	20	125.2	10.2	35.5	26.3	13.4	36.7	8.4	30.2	26.0	12.0
Th (ppm)	2.2	11	1	3	2	3	5	2	2	2	2
Pb (ppm)	6	18	2	5	6	3	7	3	6	1	8
Ga (ppm)	NA	16	11	15	17	17	18	17	18	18	15
Zn (ppm)	108	100	63	73	80	75	95	90	81	68	63
Ni (ppm)	126	32	296	131	25	82	6	86	17	23	92
Cr (ppm)	189	70	823	478	50	174	27	193	40	27	230
V (ppm)	216	336	147	226	230	169	186	225	224	209	242
Ce (ppm)	71.2	112	7	33	30	58	33	43	35	36	27
Ba (ppm)	431	1402	91	476	349	221	450	378	351	393	451
La (ppm)	34.4	51	3	18	15	26	15	19	14	13	11

Table 2. Major and Trace Element Compositions of Iranian Paleogene Trachybasalts, Basaltic Trachyandesites, Basaltic Andesites, Andesites, and Analcime-Bearing Volcanic Rocks

	Sample									
	AR5	SV4	AN3	DEHNAR1	AN5	AR3	QM2	NA3	TA5	TRD5
Latitude (WGS84)	34.31207	35.26700	33.12397	34.30428	33.13792	34.30428	34.08575	32.22457	36.22677	35.47757
Longitude (WGS84)	51.23790	50.09178	52.53003	51.17087	52.54782	51.17087	50.52168	53.25290	50.58443	54.31718
Lithology	Trachybasalt	Basaltic trachyandesite	Basaltic andesite	Basaltic andesite	Andesite	Andesite	Andesite	Analcime trachyandesite	Analcime phonotephrite	Analcime tephriphonolite
SiO_2 (%)	46.87	52.48	53.02	54.99	59.27	59.31	58.04	55.27	52.21	54.04
TiO_2 (%)	1.73	1.00	1.09	1.44	1.10	1.32	0.97	0.73	0.86	0.90
Al_2O_3 (%)	16.52	17.22	17.77	16.36	16.20	15.21	17.43	20.66	19.64	17.74
Fe_2O_3 (%)	11.30	8.04	8.41	9.38	8.31	10.38	7.68	5.77	7.91	7.51
MnO (%)	0.26	0.15	0.15	0.11	0.15	0.21	0.12	0.13	0.16	0.14
MgO (%)	6.80	7.28	6.13	1.62	2.81	2.92	3.43	1.79	2.75	2.37
CaO (%)	10.49	7.16	8.42	10.13	5.48	3.72	7.84	5.05	7.11	6.57
Na_2O (%)	3.11	3.96	3.46	3.84	3.78	3.72	3.00	4.51	3.89	3.73
K_2O (%)	2.16	1.87	1.13	1.56	2.18	2.43	1.31	5.24	4.64	6.08
P_2O_5 (%)	0.51	0.47	0.33	0.33	0.31	0.39	0.17	0.56	0.78	0.60
Total (%)	99.75	99.63	99.91	99.76	99.59	99.61	99.99	99.71	99.95	99.68
Nb (ppm)	46.7	21.4	14.6	8.7	9.2	11.3	2.4	9.4	14.5	15.2
Zr (ppm)	126	201	115	200	157	257	56	157	158	202
Y (ppm)	20.5	21.1	21.6	36.1	26.4	47.0	23.2	20.0	21.5	18.8
Sr (ppm)	866	583	426	208	444	190	365	932	1235	1410
U (ppm)	0	0	0	2	1	2	0	1	0	0
Rb (ppm)	51.1	37.9	17.5	46.5	62.8	68.4	14.2	189.6	165.4	126.5
Th (ppm)	3	7	2	6	10	8	1	12	14	12
Pb (ppm)	139	9	5	5	11	8	4	30	29	28
Ga (ppm)	16	16	17	17	17	17	22	17	17	19
Zn (ppm)	231	70	72	166	66	299	89	72	69	70
Ni (ppm)	50	139	84	9	4	1	10	5	11	10
Cr (ppm)	134	242	264	63	51	11	38	10	39	22
V (ppm)	188	130	160	243	151	148	276	83	143	165
Ce (ppm)	53	59	33	40	51	52	15	57	87	82
Ba (ppm)	1041	639	363	334	496	651	199	1362	1616	819
La (ppm)	26	31	14	16	22	21	2	28	45	38

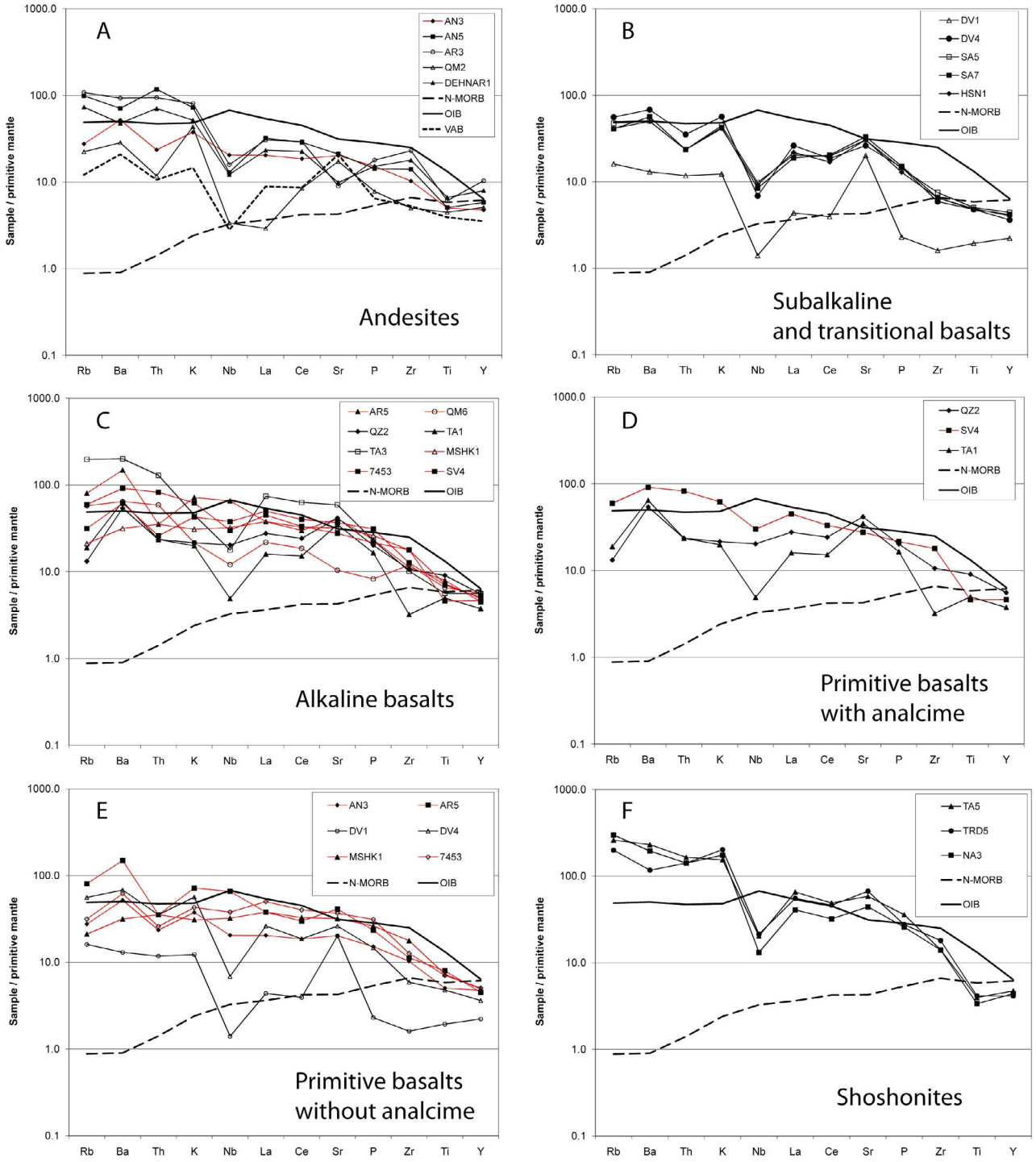

Figure 6. Primitive mantle normalized trace element diagrams. Eocene samples shown in black, and Oligocene shown in red. (a) Andesites, (b) subalkaline and transitional basalts, (c) alkaline basalts, (d) primitive basalts with analcime, (e) primitive basalts without analcime, (f) shoshonites. Primitive mantle, N-MORB, and OIB values from *Sun and McDonough* [1989]. Volcanic arc basalt (VAB) values from *Hickey et al.* [1986].

5.2. Geochemical Attributes of Flare-up and Post-Flare-up Volcanism

[25] The transfer of incompatible elements from subducting slabs to the mantle wedge is thought to be the cause of the distinctive trace element composition of arc volcanism (Figure 6) [e.g., *Pearce and Cann*, 1973; *Gill*, 1981]. The most common traits of arc volcanism are enrichment, relative to midocean ridge basalts (MORB), of large-ion lithophile elements (LILE) and the relative depletion of high field strength elements (HFSE) such as Ti, Y, Zr, Nb.

Enrichment of LILE is attributed to the addition of these water-soluble elements by fluids derived from the dehydration of the subducted slab [e.g., *Tatsumi et al.*, 1986], while depletion of the generally fluid-immobile HFSE is thought to reflect a preexisting depletion within the mantle wedge [e.g., *McCulloch and Gamble*, 1991; *Woodhead et al.*, 1993; *Elliott*, 2004].

[26] From a practical perspective, trace element compositions of volcanic rocks may not provide any meaningful information about mantle compositions if those rocks did not originate from mantle melts, or if extensive assimilation and fractional crystallization have occurred [e.g., *DePaolo*, 1981; *Dungan and Davidson*, 2004]. Because the trace element composition of bulk continental crust [*Taylor and McLennan*, 1985] is quite similar to the composition of typical arc magmas, extensive assimilation of crustal material can impart an "arc signature" to melts regardless of their original composition. Assuming that assimilation will lead to more silicic compositions, the problem can be minimized to some degree by filtering out all but the most primitive samples. Geochemical criteria developed by *Collins* [2002] were used to screen out samples that are the most likely to have been affected by crustal contamination and fractional crystallization. Samples that meet these criteria (<53 wt % SiO_2, >5 wt % MgO, >130 ppm Cr, ≥50 ppm Ni) may still be somewhat removed from mantle compositions, but are nevertheless sufficiently "primitive" to provide insight into mantle compositions (Figures 6d and 6e). Nine of our samples (7453, AN3, AR5, DV1, DV4, MSHK1, QZ2, SV4, and TA1) meet these criteria, and sample AN3 has also been included in this group despite containing 53.02 wt % SiO_2 because it meets the other geochemical criteria. Three of the basalts within the subset (SV4, TA1, and QZ2; Figure 6d) contain analcime in their groundmass, and we distinguish them from the other samples because we suspect that their original trace element compositions may have been altered during zeolite formation [*Prelević et al.*, 2004].

[27] Trace element data from the primitive and unaltered basalts suggest a key geochemical distinction between the Eocene and Oligocene samples (Figure 6e). Two samples from Late Eocene gabbros that intrude the Karaj Formation in the Alborz Mountains have typical arc characteristics, in particular prominent Nb depletions, perhaps the single most distinctive trace element characteristic of arc magmatism [*Gill*, 1981]. Although there are only two Eocene samples in this subset of primitive basalts, the trace element patterns of all of the Eocene andesites (Figure 6a) and Eocene shoshonites (Figure 6f) have Nb depletions. In short, the trace element composition of Eocene magmatism is typical of continental arcs, a finding in agreement with the vast majority of previous geochemical studies conducted on Iranian Eocene volcanism [e.g., *Jung et al.*, 1974; *Berberian et al.*, 1982; *Ghorbani*, 2006; *Omrani et al.*, 2008]. However, in contrast to Eocene volcanism, the Oligocene samples we analyzed (which are from basalts in the lower part of the Qom Formation/Gand Ab limestones and mafic dikes intruding the Eocene stratigraphy) have overall flat trace element patterns and do not have depletions in Nb. These features are similar in many ways to oceanic island basalts (OIB) (Figure 6e), and we refer to this type of magmatism below as "asthenosphere derived." In terms of geochemical and petrological characteristics, Oligocene basalts differ from the typical compositions of lavas erupted during the Paleocene-Eocene flare-up in two fundamental ways. First, Oligocene lavas are often primitive basalts, whereas Eocene volcanism was of wide-ranging composition but seldom included primitive mafic lavas. Second, the Oligocene basalts exhibit fewer of the classic geochemical traits of arc volcanism, i.e., Nb and Zr depletions and distinct positive Sr spikes, that are usually observed for the Eocene phase of volcanism. Assuming that the compositions of these basalts are, in fact, related to the compositions of their source, the difference in trace element patterns implies that the source of magmatism changed in the early Oligocene.

[28] Geochronological data place some constraints on the timing of the transition from "arc-like" to asthenosphere-derived volcanism, although it is quite possible that the change was not synchronous over all of Iran. Sample 7453, an Oligocene basalt flow at the base of the Gand Ab limestones in the Alborz Mountains, has trace element characteristics which resemble OIB (Figure 6e) and is stratigraphically equivalent to a basalt with an $^{40}Ar/^{39}Ar$ age of 32.7 ± 0.3 Ma [*Guest et al.*, 2007b]. Comparison of this date with the $^{40}Ar/^{39}Ar$ biotite age of 37.2 ± 0.38 Ma from the gabbros that intrude the Karaj Formation (equivalent in age to samples DV1 and DV4 which have typical arc trace element compositions; Figure 6e) suggests that the transition in magma sources occurred between 37 and 33 Ma. In terms of field relationships, the later period of asthenosphere-derived magmatism often occurs as basalt flows just below and within the Qom Formation, as well as mafic subvolcanic intrusions. Some of the intrusions into the Karaj Formation, such as those represented by samples DV1 and DV4, are slightly older and are part of the earlier period of magmatism with typical arc characteristics. Although additional fieldwork is required in order to fully establish the crosscutting relationships between these intrusions and overlying formations, the late Eocene-early Oligocene Lower Red Formation seems to be the stratigraphic interval that separates underlying volcanic rocks with typical arc trace element compositions from overlying asthenosphere-derived volcanism (Figure 7).

[29] Finally, Tertiary shoshonites have been widely described in Iran [e.g., *Alberti et al.*, 1979; *Amidi et al.*, 1984; *Kazmin et al.*, 1986; *Aftabi and Atapour*, 2000], and three of our new samples (TRD5, NA3, and TA5) meet the geochemical definition of shoshonite from *Morrison* [1980]. These samples are Eocene, form an outlying group on a TAS diagram (Figure 5e), and contain analcime. The petrological significance of shoshonites and widespread analcime in Iranian arc rocks is a complex issue beyond the scope of this paper. However, a relevant observation is that the Eocene shoshonites analyzed in this study have trace element compositions typical of continental arcs, most notably strong Nb depletions (Figure 6f).

5.3. Eocene Tectonic Regime

[30] Iran is currently experiencing N-S shortening [e.g., *Vernant et al.*, 2004] and probably has been since the collision of Arabia with Eurasia. Geologic evidence of past tectonic regimes, which may have been something other than contractile, are therefore obscured in Iran by Neogene shortening. In recent years, Eocene metamorphic core complexes have been recognized in central and east central

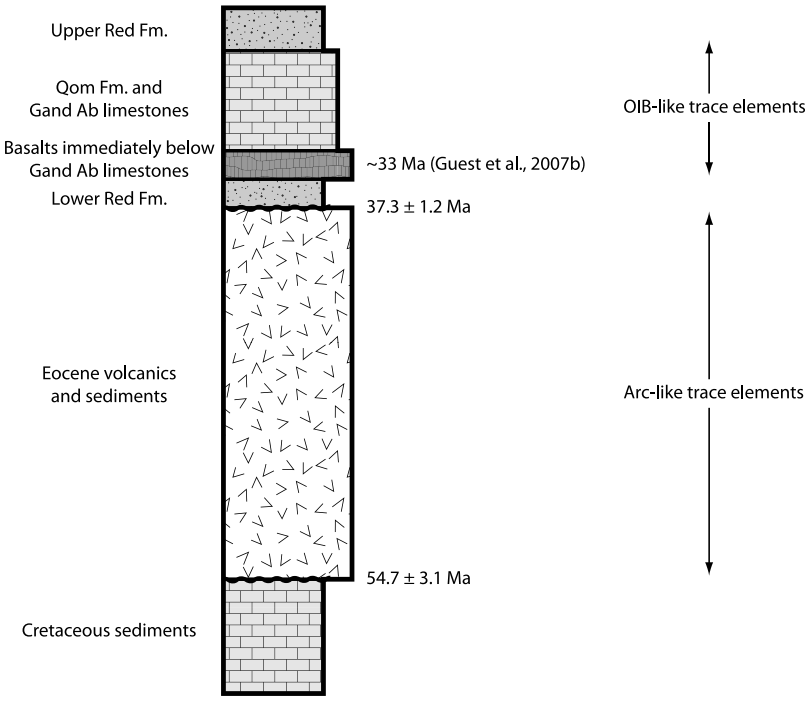

Figure 7. Generalized Tertiary stratigraphy of Iran showing key radiometric age constraints.

Iran [*Moritz et al.*, 2006; *Kargaran et al.*, 2006; *Verdel et al.*, 2007]. Very similar geologic structures in the western United States have been interpreted as evidence of large-magnitude crustal extension [e.g., *Coney*, 1980; *Armstrong*, 1982]. Eocene normal faults have been identified in the Alborz Mountains [*Guest et al.*, 2006a], and stratigraphic evidence of Eocene subsidence in the Alborz Mountains and central Iran has been interpreted in terms of Eocene extension [*Brunet et al.*, 2003; *Hassanzadeh et al.*, 2004; *Vincent et al.*, 2005; *Guest et al.*, 2007b; *Morley et al.*, 2009]. In the major Paleogene outcrops in Iran, the presence of shallow marine sediments interbedded through essentially the entire thickness of Paleogene volcanic accumulations (Figures 3 and 4) [*Stöcklin*, 1968; *Berberian and King*, 1981; *Emami*, 1991], as well as evidence of submarine volcanism [e.g., *Förster et al.*, 1972; *Amidi et al.*, 1984; *Spies et al.*, 1984; *Hassanzadeh*, 1993], suggest synvolcanic subsidence. Furthermore, some Paleogene sediments in southern Iran have clearly been affected by domino-style normal faulting [*Tillman et al.*, 1981]. Thus, there is a growing body of evidence that much, if not all of Iran was undergoing extension during at least part of the Eocene. As discussed in detail below, the temporal association of the magmatic flare-up with a period of extensional tectonism raises the question of how the two may be related.

5.4. Space-Time Variations of Iranian Arc Magmas

[31] Although Paleogene volcanism is the most obvious manifestation of Neotethyan subduction beneath Iran, paleogeographic reconstructions [e.g., *Dercourt et al.*, 1986; *Stampfli and Borel*, 2002] suggest that the flare-up was preceded by roughly 150 Myr of subduction. As described above, the earliest magmatic evidence for Neotethys subduction are Triassic plutons in the Sanandaj-Sirjan zone of SW Iran. These intrusions, together with Jurassic plutons in the same region, are remnants of the Mesozoic continental arc [e.g., *Berberian and Berberian*, 1981; *Arvin et al.*, 2007; *Omrani et al.*, 2008]. Cretaceous magmatic activity in Iran was limited, but, with the exception of Cretaceous volcanic rocks in the northwesternmost part of the Sanandaj-Sirjan zone [*Azizi and Jahangiri*, 2008], magmatism apparently migrated to the northern part of Iran during the Cretaceous (Figure 1). The distribution of Late Triassic-Jurassic arc remnants in the Sanandaj-Sirjan zone relative to Cretaceous arc rocks in northern Iran suggests that the axis of magmatism shifted inland by mid-Cretaceous time. Subsequent Tertiary volcanism was distributed over a large area (encompassing the Urumieh-Dokhtar belt, the Alborz Mountains, large parts of eastern Iran, and many relatively small locations in central Iran) but generally occurred between Cretaceous igneous rocks to the north and Triassic-Jurassic plutons to the south (Figure 1). As described in more detail below, we suggest that long-lived subduction along or south of what is now the Main Zagros reverse fault was responsible for all of these elements of the Late Triassic to Miocene magmatic arc system of Iran. In other words, the record of arc volcanism in Iran encompasses not only the well defined belt of Paleogene calc-alkaline volcanics in the Urumieh-Dokhtar arc, but is widespread across Iran and spans roughly 175 Myr.

5.5. Mechanism for the Iranian Tertiary Flare-up

[32] In this section we evaluate the plausibility of the following mechanisms for generating the Paleogene flare-up: change in subduction rate, change in subduction angle, slab melting, and back-arc basin development/rifting. We evaluate these explanations in light of the key observations described above, namely, (1) the duration of the Paleogene

flare-up represents approximately 10% of the entire duration of Neotethyan subduction beneath Iran; (2) Eocene arc-type volcanism was followed by Oligocene asthenosphere-derived mafic magmatism; (3) the flare-up was accompanied by normal faulting, thousands of meters of subsidence, and was broadly coincident in time and space with the formation of metamorphic core complexes; and (4) Paleogene volcanism occurred 100 to 500 km inland from the remnants of the Late Triassic-Jurassic arc.

5.5.1. Changes in Subduction Rate

[33] Increased subduction rate would add a proportionally larger supply of hydrous fluids to the subduction zone per unit time, presumably leading to an increase in melt production as predicted by simple models of flux melting. *Kazmin et al.* [1986] proposed an explanation analogous to this for the Iranian flare-up, while *Takin* [1972], *Pazirandeh* [1973], and *Hassanzadeh* [1993] held the opposite view and argued that subduction slowed in the Eocene because of diminished spreading in the Indian Ocean, leading to extension and volcanism within the Iranian arc. Kinematic reconstructions of Arabia-Eurasia convergence offer a direct means of evaluating these hypotheses. These plate reconstructions show that the rate of convergence between Arabia and Eurasia was 2–3 cm/yr from ~56 to 20 Ma [*McQuarrie et al.*, 2003], implying, at the least, that the end of the pulse was not coincident with a change in subduction rate. In the mid-Cretaceous, Arabia-Eurasia convergence rate is believed to have climbed as high as approximately 6–7 cm/yr for roughly 25 Myr, but then returned to relatively slow values (~3 cm/yr) by 70 Ma [*Agard et al.*, 2006, 2007]. Therefore, although there are no convergence rate estimates available for the period immediately preceding the flare-up, existing data suggest that Arabia-Eurasia convergence was 3–3.5 cm/yr during both the latest Cretaceous and throughout the Eocene [*McQuarrie et al.*, 2003; *Agard et al.*, 2007]. Based on these reconstructions, there seems to be no evidence that the flare-up was triggered by a change in convergence rate.

5.5.2. Changes in Subduction Angle

[34] It has been proposed that the great width of the Paleogene arcs in central and northern Iran relative to the Mesozoic arc preserved in the Sanandaj-Sirjan zone of southwestern Iran reflects an early Tertiary episode of flat slab subduction [*Berberian and Berberian*, 1981; *Shahabpour*, 2007]. By analogy with the Laramide orogeny of western North America and the modern southern Andes [e.g., *Bird*, 1984; *Jordan and Allmendinger*, 1986], flat slab subduction would have been accompanied by regional compression. For the Laramide, it has been suggested that flat slab subduction could remove the lithospheric mantle from the overriding plate and trigger melting via upwelling of asthenospheric mantle in the wake of slab removal [*Bird*, 1988]. This model, as applied to Iran, could therefore explain Oligocene magmas which seem to be sourced from the asthenosphere. However, it is at odds with the evidence summarized above for widespread subsidence and tectonic extension during the Eocene. Based on these observations, it is unlikely that an episode of flat slab subduction centered on Eocene time was responsible for the flare-up.

[35] However, there is some evidence that flat slab subduction may have occurred during the Cretaceous. First, some Cretaceous magmatism occurred in the northern part of Iran (Figure 1), in contrast to earlier Mesozoic plutonism that was concentrated in the southwestern part of the country, i.e., the relict magmatic arc in the Sanandaj-Sirjan zone. The fact that Cretaceous volcanism was not widespread is similar to the pattern observed in the Laramide of the western United States, where magmatism during the flat slab phase was neither voluminous nor widespread in comparison with the earlier coastal arc batholiths or the post-Laramide ignimbrite flare-up. Second, a regional unconformity separating Cretaceous sediments from overlying Paleogene volcanic rocks implies a phase of contractional deformation that preceded the Eocene flare-up [e.g., *Stöcklin*, 1968]. This event may also be reflected in the Late Cretaceous to Paleocene cooling of a middle Cretaceous pluton in the Alborz Mountains [*Guest et al.*, 2006b] and Late Cretaceous folding and thrust faulting in the Sanandaj-Sirjan zone [e.g., *Tillman et al.*, 1981]. We therefore suggest that the Cretaceous inland shift in magmatism and roughly contemporaneous phase of compressional tectonism may have resulted from a period of flat slab subduction.

5.5.3. Slab Melting

[36] In recent years geochemical evidence has emerged from some arcs that suggests melting of oceanic crust in the downgoing slab may play a role in generating magmatism and, in particular, adakitic volcanism [e.g., *Defant and Drummond*, 1990; *Gómez-Tuena et al.*, 2007]. Slab melting has been proposed as a mechanism for generating Tertiary volcanism in Iran [*Aftabi and Atapour*, 2000; *Omrani et al.*, 2008]. None of the samples analyzed during this study are adakites based on the geochemical criteria specified by *Defant and Drummond* [1990], although there are Neogene adakites in the Urumieh-Dokhtar arc [*Jahangiri*, 2007; *Omrani et al.*, 2008]. Geochemical data taken as a whole do not support Paleogene slab melting, nor does slab melting explain the inland position of the Tertiary arc or synvolcanic extension and subsidence.

5.5.4. Rifting/Back-Arc Basin Development

[37] *Kazmin et al.* [1986] suggested that Eocene volcanism in Iran and throughout the Middle East and Mediterranean regions was related to the opening of back-arc basins. This mechanism accounts for many of the characteristics of the Eocene flare-up: the inland position of the Urumieh-Dokhtar belt relative to the Late Triassic-Jurassic arc, synextensional volcanism, development of shallow submarine basins, and the asthenosphere-like geochemical affinity of the Oligocene basalts. However, Eocene volcanism, which was much more voluminous than Oligocene volcanism, had trace element compositions that are typical of arcs, not back arcs, and accumulated in the same basins as the Oligocene basalts. These first-order observations of the magmatic flare-up can be most simply explained as resulting from a hybrid of two common end-member mechanisms for generating volcanism: hydration of the mantle wedge by slab fluids as in subduction zones and decompression melting as in midocean ridges [*Plank and Langmuir*, 1988; *Pearce and Parkinson*, 1993; *Sisson and Bronto*, 1998; *Conder et al.*, 2002; *Gaetani and Grove*, 2004].

[38] In the model outlined below, the pre-flare-up supply of fluids derived from slowly subducting Neotethyan oceanic crust was sufficient to partially hydrate and alter the trace element composition of the mantle wedge, but insufficient to induce significant magmatism until extension and

decompression melting began. As a result, trace element compositions of Eocene lavas related to decompression, but derived from a metasomatized source, are indistinguishable from volcanism in other arcs where flux-melting predominates.

5.6. Tectonic Model for the Eocene Magmatic Flare-up

[39] We propose the following four-stage model for the Eocene magmatic flare-up and subsequent Oligocene magmatism, which is broadly similar to the model of *Humphreys et al.* [2003] for the mid-Tertiary flare-up event in the western United States. In the first stage, relatively steep slab descent preconditioned arc lithosphere in the region immediately north of the Arabia-Eurasia suture (Figure 8a). In the second stage, beginning no later than Aptian-Albian time, the slab flattened, generating presumed arc-related magmas in the Alborz Mountains and in north central Iran and, ultimately, Late Cretaceous contractile tectonics throughout much of Iran to the north of the suture. During this stage, preconditioning of the upper mantle spread northward to encompass the Alborz Mountains and north central Iran (Figure 8b).

[40] In the third stage, Eocene extension and crustal thinning accompanying slab rollback generated decompression melting of the preconditioned mantle. Hydrated peridotite in the lithospheric mantle partially melted due to the combined effects of decompression and heating from the underlying upwelling asthenosphere. Both the lithospheric and asthenospheric mantle would have undergone partial melting during this period (Figure 8c). Melting was particularly extensive in the HFSE-depleted lithospheric mantle during this stage because it had been partially hydrated during the extended interval of subduction that preceded the flare-up. Thick volcanic and sedimentary successions accumulated in continental and shallow submarine extensional basins.

[41] In the fourth stage, beginning in the Oligocene, upwelling asthenosphere replaced the thinned lithosphere (Figure 8d). Comparatively limited melting of the asthenospheric source was responsible for Oligocene magmatism, in much the same fashion as widely proposed for generating back-arc basin basalts [e.g., *Gribble et al.*, 1998]. Basalts were predominant during this period because the thinned crust contributed relatively little contamination and was an ineffective density barrier to primitive magmas [*Plank and Langmuir*, 1988; *Glazner and Ussler*, 1989]. Given stratigraphic evidence for continued extension and subsidence during deposition of the Oligo-Miocene Qom Formation [e.g., *Hassanzadeh and Fakhari*, 1997], the late Eocene-early Oligocene transition from extensive arc magmatism to limited asthenosphere-derived volcanism may have occurred when the supply of fertile, preconditioned lithospheric mantle was exhausted. Subsequent post-late Miocene (i.e., postcollisional) adakitic volcanism in the Urumieh-Dokhtar arc may be related to slab break-off, as suggested by *Jahangiri* [2007], *Omrani et al.* [2008], and *Hassanzadeh et al.* [2009].

[42] The overall Paleocene to Miocene magmatic history of Iran thus began with the accumulation of late Paleocene-early Eocene volcanic and sedimentary strata in extensional subsiding submarine basins developed inland of the Mesozoic arc. Marine deposition continued in these basins until at least early Oligocene time. Although continental red beds of the Lower Red Formation suggest that marine deposition was locally interrupted, the regionally extensive Oligocene-Miocene Qom Formation indicates that marine conditions prevailed to the end of early Miocene time in much of Iran.

[43] Accompanying the collision of Arabia with Eurasia, the Paleogene basins were inverted [*Emami*, 1991; *Guest et al.*, 2007a; *Morley et al.*, 2009], and are still being uplifted as the collision continues. A well-documented example of basin inversion is near Saghand in eastern Iran (Figure 1) [*Ramezani and Tucker*, 2003; *Verdel et al.*, 2007], where synextensional middle Eocene volcanic and sedimentary strata were deposited in supradetachment basins [see, e.g., *Friedmann et al.*, 1994] during core complex formation and were subsequently exhumed by ~N-S shortening at ~20 Ma [*Verdel et al.*, 2007]. The two largest extensional basins in terms of area are the elongate basins of Paleogene strata in the Alborz Mountains and Urumieh-Dokhtar belt. The proposed Iranian history of slab rollback, basin formation, asthenosphere-derived volcanism, and subsequent basin inversion may represent one cycle in the growth of an extensional accretionary orogen, according to the definition of *Collins* [2002]. Abundant Eocene and Oligocene volcanism in the Lut block of eastern Iran (Figure 1) may have developed in a similar tectonic setting as suggested by *Jung et al.* [1984], although our data do not bear directly on that region.

5.7. Implications for Other Arcs

[44] Similar models for extensional flare-up magmatism have been suggested in several locations. A comparable explanation has been proposed for the development of Cenozoic and Mesozoic continental rift magmatism in western North America [*Lawton and McMillan*, 1999]. There, a similar transition occurred from an earlier phase of voluminous arc magmatism to a later period of relatively restricted OIB-type volcanism. Cretaceous-early Tertiary magmatism in the Coast Mountains batholith of northwestern North America seems to have been characterized by a transition from "arc-like" magmatism during compression to a later period of decompression melting accompanying extension [*Hollister and Andronicos*, 2006]. Slab rollback following a period of flat slab subduction may have triggered the mid-Tertiary ignimbrite flare-up in the western United States [*Humphreys*, 1995; *Humphreys et al.*, 2003]. In the eastern Mediterranean region, it has been argued that an analogous transition was related to extension of the Aegean and Anatolian plates during slab rollback [e.g., *Agostini et al.*, 2007]. In the Mexican volcanic belt, decompression melting of asthenospheric mantle may be responsible for Neogene extension-related volcanism [*Wallace and Carmichael*, 1999; *Verma*, 2002; *Blatter et al.*, 2007]. Indeed, a number of similarities between the Iranian arc and the western part of the central Mexican arc are noteworthy. Like subduction of Neotethys below Arabia for a significant part of its history, subduction of the Rivera plate beneath Mexico has been quite slow (1–5 cm/yr) over much of the last 10 million years [*DeMets and Traylen*, 2000]. Some Pliocene-Quaternary lavas from the western part of the Mexican arc were erupted at particularly high rates and have OIB geochemical attributes [*Wallace et al.*, 1992]. On a TAS diagram, some 1200 analyses from the

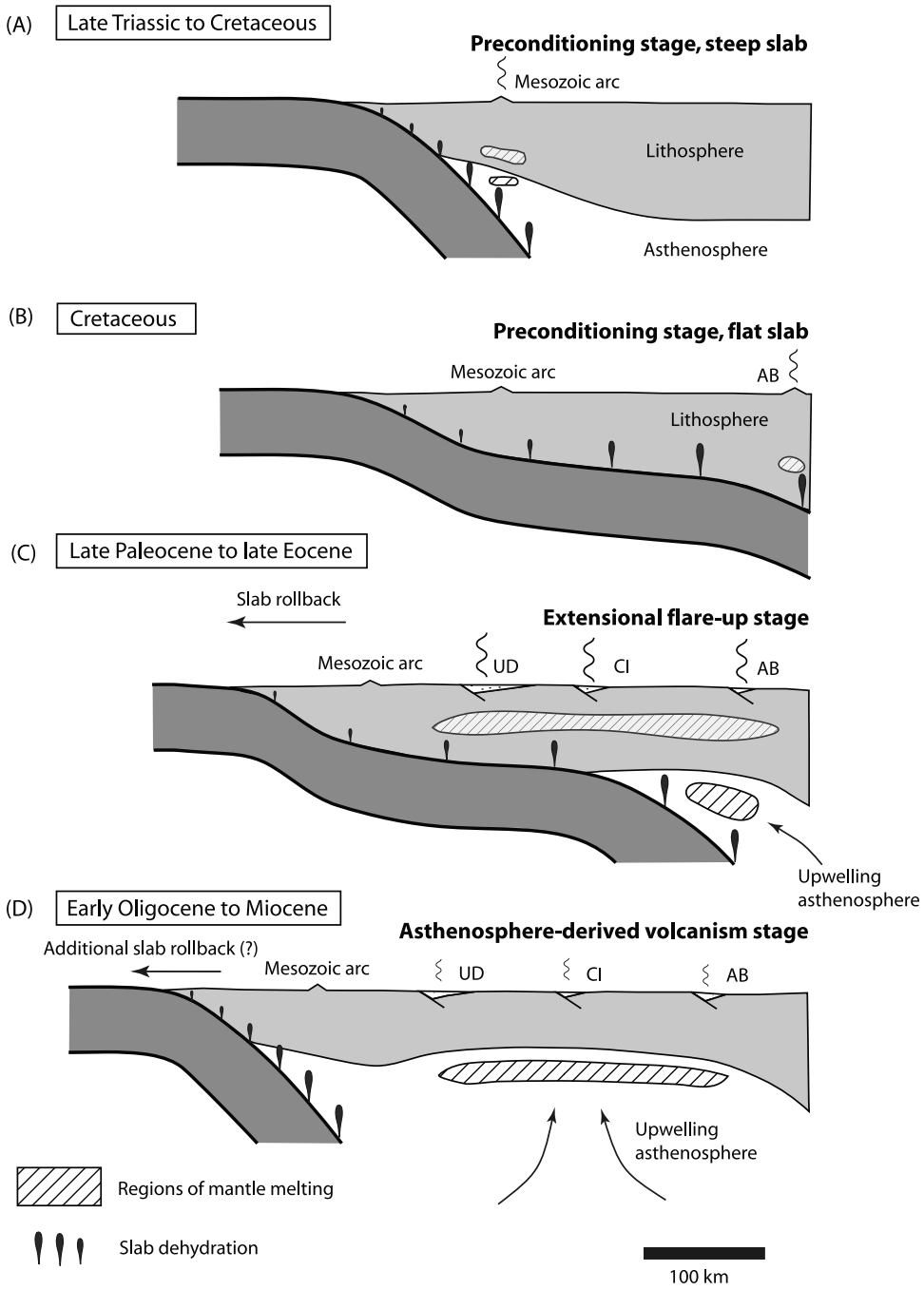

Figure 8. Summary of the development of the Iranian Eocene flare-up and subsequent asthenosphere-derived Oligocene magmatism. (a) Late Triassic to Cretaceous slow subduction generated limited magmatism within the Sanandaj-Sirjan zone. (b) Cretaceous flat slab subduction shifted the locus of magmatism to the Alborz Mountains. During this and the earlier stage, lithospheric mantle beneath the overriding plate was preconditioned by dehydration of subducted Neotethyan oceanic crust. (c) Late Paleocene to late Eocene slab rollback extended and thinned the overriding plate, leading to decompression melting of preconditioned lithospheric mantle and the formation of metamorphic core complexes and elongate rift basins. Magmatic contributions from upwelling asthenosphere were overwhelmed during this stage by the contribution from the fertilized lithospheric mantle. (d) Extension continued during the late Oligocene to Miocene during deposition of the Qom Formation. The flare-up ended when the supply of fertile, preconditioned lithospheric mantle was exhausted, at which time asthenosphere-derived, OIB-type volcanism became dominant. Miocene Arabia-Eurasia collision ended the extensional period and inverted the rift basins. Abbreviations: UD, Urumieh-Dokhtar magmatic belt; AB, Alborz Mountains; CI, central Iranian Eocene volcanics between Urumieh-Dokhtar and the Alborz Mountains.

Mexican volcanic belt, compiled from the GEOROC database, are scattered toward high alkalinity, similar to Iranian Tertiary volcanism (Figure 5f). The Mexican volcanic belt includes analcime-bearing Neogene shoshonites [*Luhr and Kyser*, 1989; *Karlsson and Clayton*, 1991], which seem similar to the analcime-bearing shoshonites of Iran. Not surprisingly, the unusual compositions of the Mexican volcanics have spawned a wide range of tectonic and petrologic explanations, including rifting [*Lange and Carmichael*, 1991; *Verma*, 2002], slab melting [*Gómez-Tuena et al.*, 2007], interaction with a mantle plume [*Márquez et al.*, 1999], and slab break-off [*Ferrari*, 2004]. Despite these contrasting interpretations, there seems to be general agreement that extension played a role in generating volcanism associated within grabens in the western part of the belt [e.g., *Lange and Carmichael*, 1991; *Wallace et al.*, 1992].

[45] These similarities suggest that the Mexican volcanic belt, and perhaps also the eastern Mediterranean region, may be active analogs for Iranian Paleogene volcanism. Although the total volume of volcanism during the Iranian flare-up has not been precisely quantified, a simple calculation based on outcrop extent and average thickness suggests that the volume of erupted material is likely of order 10^6 cubic kilometers, so the Iranian example may ultimately stand as a particularly impressive example of an extensional flare-up. Average accumulation rate over the entire duration of the flare-up is of order 0.1 mm/yr, although during periods of peak productivity the rate may have climbed to over 1 mm/yr [*McQuarrie et al.*, 2003]. Extensive preconditioning of the mantle wedge during subduction preceding the flare-up, which we infer may have included 50 Myr in a flat slab regime, could be a key factor in explaining the large amounts of extension-related volcanism. Slow subduction rate, coupled with the relatively large consumption of oceanic crust necessary to close Neotethys from Iran's position in Gondwana, may have been a particularly effective combination that facilitated extraordinary mantle fertilization and the ensuing Paleocene flare-up.

[46] **Acknowledgments.** We acknowledge analytical assistance from Axel Schmitt of the UCLA Keck ion microprobe facility, Terry Spell of the Nevada Isotope Geochronology Lab, and Mike Rhodes of the University of Massachusetts. This research was supported by NSF grant EAR-0511054 awarded to B. Wernicke, grant EAR-0337775 awarded to G. Axen and B. Horton, and the Gordon and Betty Moore Foundation. The ion microprobe facility at UCLA is partly supported by a grant from the Instrumentation and Facilities Program, Division of Earth Sciences, National Science Foundation. Discussions with Gary Axen, John Eiler, Jahandar Ramezani, and Danny Stockli contributed significantly to the development of ideas in this paper. We appreciate constructive reviews from Philippe Agard, Mihai Ducea, Robert Miller, Chris Morley, and an anonymous reviewer. This is Caltech Tectonics Observatory contribution 148.

References

Aftabi, A., and H. Atapour (2000), Regional aspects of shoshonitic volcanism in Iran, *Episodes*, *23*, 119–125.

Agard, P., J. Omrani, L. Jolivet, and F. Mouthereau (2005), Convergence history across Zagros (Iran): Constraints from collisional and earlier deformation, *Int. J. Earth Sci.*, *94*, 401–419, doi:10.1007/s00531-005-0481-4.

Agard, P., P. Monié, W. Gerber, J. Omrani, M. Molinaro, B. Meyer, L. Labrousse, B. Vrielynck, L. Jolivet, and P. Yamato (2006), Transient, synobduction exhumation of Zagros blueschists inferred from P-T, deformation, time, and kinematic constraints: Implications for Neotethyan wedge dynamics, *J. Geophys. Res.*, *111*, B11401, doi:10.1029/2005JB004103.

Agard, P., L. Jolivet, B. Vrielynck, E. Burov, and P. Monié (2007), Plate acceleration: The obduction trigger?, *Earth Planet. Sci. Lett.*, *258*, 428–441, doi:10.1016/j.epsl.2007.04.002.

Agostini, S., C. Doglioni, F. Innocenti, P. Manetti, S. Tonarini, and M. Y. Savaşçin (2007), The transition from subduction-related to intraplate Neogene magmatism in the western Anatolia and Aegean area, in *Cenozoic Volcanism in the Mediterranean Area*, edited by L. Beccaluva, G. Bianchini, and M. Wilson, *Spec. Pap. Geol. Soc. Am.*, *418*, 1–15, doi:10.1130/2007.2418(01).

Alavi, M., and A. Hushmandzādeh (1976), Geological map of the Torud quadrangle, scale 1:250,000, Geol. Surv. of Iran, Tehran.

Alberti, A., P. Comin-Chiaramonti, G. Di Battistini, S. Sinigoi, and M. Zerbi (1979), Upper Eocene to early Oligocene shoshonitic volcanism in eastern Azerbaijan, *Neues Jahrb. Mineral Abh.*, *134*, 248–264.

Allen, M. B., and H. A. Armstrong (2008), Arabia-Eurasia collision and the forcing of mid-Cenozoic global cooling, *Palaeogeogr. Palaeoclimatol. Palaeoecol.*, *265*, 52–58, doi:10.1016/j.palaeo.2008.04.021.

Amidi, S. M., and R. Michel (1985), Cenozoic magmatism of the Surk area (central Iran) stratigraphy, petrography, geochemistry and their geodynamic implications, *Geol. Alp.*, *61*, 1–16.

Amidi, S. M., M. H. Emami, and R. Michel (1984), Alkaline character of Eocene volcanism in the middle part of central Iran and its geodynamic situation, *Geol. Rundsch.*, *73*, 917–932, doi:10.1007/BF01820882.

Annells, R. N., R. S. Arthurton, R. A. Bazley, and R. G. Davies (1975), Explanatory text of the Qazvin and Rasht quadrangles map, *Quadrangles E3 and E4*, 94 pp., Geol. Surv. of Iran Geol., Tehran.

Armstrong, R. L. (1982), Cordilleran metamorphic core complexes—From Arizona to southern Canada, *Annu. Rev. Earth Planet. Sci.*, *10*, 129–154, doi:10.1146/annurev.ea.10.050182.001021.

Arvin, M., Y. Pan, S. Dargahi, A. Malekizadeh, and A. Babaei (2007), Petrochemistry of the Siah-Kuh granitoid stock southwest of Kerman, Iran: Implications for initiation of Neotethys subduction, *J. Asian Earth Sci.*, *30*, 474–489, doi:10.1016/j.jseaes.2007.01.001.

Axen, G. J., P. S. Lam, M. Grove, D. F. Stockli, and J. Hassanzadeh (2001), Exhumation of the west-central Alborz Mountains, Iran, Caspian subsidence, and collision-related tectonics, *Geology*, *29*, 559–562, doi:10.1130/0091-7613(2001)029<0559:EOTWCA>2.0.CO;2.

Azizi, H., and A. Jahangiri (2008), Cretaceous subduction-related volcanism in the northern Sanandaj-Sirjan Zone, Iran, *J. Geodyn.*, *45*, 178–190, doi:10.1016/j.jog.2007.11.001.

Berberian, F., and M. Berberian (1981), Tectono-plutonic episodes in Iran, in *Zagros, Hindu Kush, Himalaya: Geodynamic Evolution*, edited by H. K. Gupta and F. M. Delany, pp. 5–32, AGU, Washington, D. C.

Berberian, F., I. D. Muir, R. J. Pankhurst, and M. Berberian (1982), Late Cretaceous and early Miocene Andean-type plutonic activity in northern Makran and central Iran, *J. Geol. Soc.*, *139*, 605–614, doi:10.1144/gsjgs.139.5.0605.

Berberian, M., and G. C. P. King (1981), Towards a paleogeography and tectonic evolution of Iran, *Can. J. Earth Sci.*, *18*, 210–265, doi:10.1139/e81-019.

Bird, P. (1984), Laramide crustal thickening event in the Rocky Mountain foreland and Great Plains, *Tectonics*, *3*, 741–758, doi:10.1029/TC003i007p00741.

Bird, P. (1988), Formation of the Rocky Mountains, western United States: A continuum computer model, *Science*, *239*, 1501–1507, doi:10.1126/science.239.4847.1501.

Blatter, D. L., G. L. Farmer, and I. S. E. Carmichael (2007), A north-south transect across the central Mexican volcanic belt at ~100°W: Spatial distribution, petrological, geochemical, and isotopic characteristics of Quaternary volcanism, *J. Petrol.*, *48*, 901–950, doi:10.1093/petrology/egm006.

Boccaletti, M., F. Innocenti, P. Manetti, R. Mazzuoli, A. Motamed, G. Pasquare, F. Radicati di Brozolo, and E. Amin Sobhani (1976), Neogene and Quaternary volcanism of the Bijar area (western Iran), *Bull. Volcanol.*, *40*, 121–132, doi:10.1007/BF02599857.

Brunet, M.-F., M. V. Korotaev, A. V. Ershov, and A. M. Nikishin (2003), The South Caspian basin: A review of its evolution from subsidence modelling, *Sediment. Geol.*, *156*, 119–148, doi:10.1016/S0037-0738(02)00285-3.

Collins, W. J. (2002), Nature of extensional accretionary orogens, *Tectonics*, *21*(4), 1024, doi:10.1029/2000TC001272.

Conder, J. A., D. A. Wiens, and J. Morris (2002), On the decompression melting structure at volcanic arcs and back-arc spreading centers, *Geophys. Res. Lett.*, *29*(15), 1727, doi:10.1029/2002GL015390.

Coney, P. J. (1978), Mesozoic-Cenozoic Cordilleran plate tectonics, in *Cenozoic Tectonics and Regional Geophysics of the Western Cordillera*, edited by R. B. Smith and G. P. Eaton, *Mem. Geol. Soc. Am.*, *152*, 33–50.

Coney, P. J. (1980), Cordilleran metamorphic core complexes: An overview, in *Cordilleran Metamorphic Core Complexes*, edited by M. D.

Crittenden Jr., P. J. Coney, and G. H. Davis, *Mem. Geol. Soc. Am.*, *153*, 7–31.

Davies, J. H., and M. J. Bickle (1991), A physical model for the volume and composition of melt produced by hydrous fluxing above subduction zones, *Philos. Trans. R. Soc. London, Ser. A*, *335*, 355–364.

Davies, J. H., and D. J. Stevenson (1992), Physical model of source region of subduction zone volcanics, *J. Geophys. Res.*, *97*, 2037–2070, doi:10.1029/91JB02571.

Defant, M., and M. Drummond (1990), Derivation of some modern arc magmas by melting of young subducted lithosphere, *Nature*, *347*, 662–665, doi:10.1038/347662a0.

DeMets, C., and S. Traylen (2000), Motion of the Rivera plate since 10 Ma relative to the Pacific and North American plates and the mantle, *Tectonophysics*, *318*, 119–159, doi:10.1016/S0040-1951(99)00309-1.

DePaolo, D. J. (1981), Trace element and isotopic effects of combined wallrock assimilation and fractional crystallization, *Earth Planet. Sci. Lett.*, *53*, 189–202, doi:10.1016/0012-821X(81)90153-9.

Dercourt, J., et al. (1986), Geological evolution of the Tethys belt from the Atlantic to the Pamirs since the Lias, *Tectonophysics*, *123*, 241–315, doi:10.1016/0040-1951(86)90199-X.

Dewey, J. F., W. C. Pitman III, W. B. F. Ryan, and J. Bonnin (1973), Plate tectonics and the evolution of the Alpine system, *Geol. Soc. Am. Bull.*, *84*, 3137–3180, doi:10.1130/0016-7606(1973)84<3137:PTATEO>2.0.CO;2.

Ducea, M. (2001), The California Arc: Thick granitic batholiths, eclogitic residues, lithospheric-scale thrusting, and magmatic flare-ups, *GSA Today*, *11*, 4–10, doi:10.1130/1052-5173(2001)011<0004:TCATGB>2.0.CO;2.

Ducea, M. N., and M. D. Barton (2007), Igniting flare-up events in Cordilleran arcs, *Geology*, *35*, 1047–1050, doi:10.1130/G23898A.1.

Dungan, M. A., and J. Davidson (2004), Partial assimilative recycling of the mafic plutonic roots of arc volcanoes: An example from the Chilean Andes, *Geology*, *32*, 773–776, doi:10.1130/G20735.1.

Dupuy, C., and J. Dostal (1978), Geochemistry of calc-alkaline volcanic rocks from southeastern Iran (Kouh-e-Shahsavaran), *J. Volcanol. Geotherm. Res.*, *4*, 363–373, doi:10.1016/0377-0273(78)90022-7.

Elliott, T. (2004), Tracers of the slab, in *Inside the Subduction Factory*, *Geophys. Monogr. Ser.*, vol. 138, edited by J. Eiler, pp. 23–45, AGU, Washington, D. C.

Emami, M. H. (1991), Explanatory text of the Qom quadrangle map, *Geol. Quadrangle E6*, Geol. Surv. of Iran, Tehran.

Fakhari, M. D., G. J. Axen, B. K. Horton, J. Hassanzadeh, and A. Amini (2008), Revised age of proximal deposits in the Zagros foreland basin and implications for Cenozoic evolution of the High Zagros, *Tectonophysics*, *451*, 170–185, doi:10.1016/j.tecto.2007.11.064.

Ferrari, L. (2004), Slab detachment control on mafic volcanic pulse and mantle heterogeneity in central Mexico, *Geology*, *32*, 77–80, doi:10.1130/G19887.1.

Förster, H., K. Fesefeldt, and M. Kürsten (1972), Magmatic and orogenic evolution of the central Iranian volcanic belt, in *24th International Geologic Congress*, edited by J. E. Armstrong and H. D. Hedberg, pp. 198–210, Int. Geol. Congr., Montreal, QC, Canada.

Friedmann, S. J., G. A. Davis, T. K. Fowler, T. Brudos, M. Parke, D. W. Burbank, and B. C. Burchfiel (1994), Stratigraphy and gravity-slide elements of a Miocene supradetachment basin, Shadow Valley, East Mojave Desert, in *Geological Investigations of an Active Margin: Geological Society of America Cordilleran Section Guidebook*, edited by S. F. McGill and T. M. Ross, pp. 302–318, San Bernardino County Mus. Assoc., Redlands, Calif.

Gaetani, G. A., and T. L. Grove (2004), Experimental constraints on melt generation in the mantle wedge, in *Inside the Subduction Factory*, *Geophys. Monogr. Ser.*, vol. 138, edited by J. Eiler, pp. 107–133, AGU, Washington, D. C.

Gans, P. B., G. A. Manhood, and E. Schermer (1989), *Synextensional Magmatism in the Basin and Range Province: A Case Study From the Eastern Great Basin*, *Spec. Pap. Geol. Soc. Am.*, *233*, 53 pp.

Gavillot, Y., G. J. Axen, D. F. Stockli, B. K. Horton, and M. D. Fakhari (2010), Timing of thrust activity in the High Zagros fold-thrust belt, Iran, from (U-Th)/He thermochronometry, *Tectonics*, *29*, TC4025, doi:10.1029/2009TC002484.

Ghorbani, M. R. (2006), Lead enrichment in Neotethyan volcanic rocks from Iran: The implications of a descending slab, *Geochem. J.*, *40*, 557–568, doi:10.2343/geochemj.40.557.

Gill, J. B. (1981), *Orogenic Andesites and Plate Tectonics*, 390 pp., Springer, Berlin.

Glazner, A. F., and W. Ussler III (1989), Crustal extension, crustal density, and the evolution of Cenozoic magmatism in the Basin and Range of the western United States, *J. Geophys. Res.*, *94*, 7952–7960, doi:10.1029/JB094iB06p07952.

Gómez-Tuena, A., C. H. Langmuir, S. L. Goldstein, S. M. Straub, and F. Ortega-Gutiérrez (2007), Geochemical evidence for slab melting in the Trans-Mexican volcanic belt, *J. Petrol.*, *48*, 537–562, doi:10.1093/petrology/egl071.

Gribble, R. F., R. J. Stern, S. Newman, S. H. Bloomer, and T. O'Hearn (1998), Chemical and isotopic composition of lavas from the northern Mariana trough: Implications for magmagenesis in back-arc basins, *J. Petrol.*, *39*, 125–154, doi:10.1093/petrology/39.1.125.

Grove, M., C. E. Jacobson, A. P. Barth, and A. Vucic (2003), Temporal and spatial trends of Late Cretaceous-early Tertiary underplating Pelona and related schist beneath southern California and southwestern Arizona, in *Tectonic Evolution of Northwestern Mexico and the Southwestern USA*, edited by S. E. Johnson et al., *Spec. Pap. Geol. Soc. Am.*, *374*, 381–406.

Guest, B., G. J. Axen, P. S. Lam, and J. Hassanzadeh (2006a), Late Cenozoic shortening in the west-central Alborz Mountains, northern Iran, by combined conjugate strike-slip and thin-skinned deformation, *Geosphere*, *2*, 35–52, doi:10.1130/GES00019.1.

Guest, B., D. F. Stockli, M. Grove, G. J. Axen, P. S. Lam, and J. Hassanzadeh (2006b), Thermal histories from the central Alborz Mountains, northern Iran: Implications for the spatial and temporal distribution of deformation in northern Iran, *Geol. Soc. Am. Bull.*, *118*, 1507–1521, doi:10.1130/B25819.1.

Guest, B., A. Guest, and G. Axen (2007a), Late Tertiary tectonic evolution of northern Iran: A case for simple crustal folding, *Global Planet. Change*, *58*, 435–453, doi:10.1016/j.gloplacha.2007.02.014.

Guest, B., B. K. Horton, G. J. Axen, J. Hassanzadeh, and W. C. McIntosh (2007b), Middle to late Cenozoic basin evolution in the western Alborz Mountains: Implications for the onset of collisional deformation in northern Iran, *Tectonics*, *26*, TC6011, doi:10.1029/2006TC002091.

Haghipour, A., and A. Aghanabati (Comps.) (1985), Geological map of Iran, scale 1:2,500,000, Geol. Surv. of Iran Min. of Mines and Metals, Tehran.

Haghipour, A., H. Taraz, and F. Vahdati Daneshmand (Comps.) (1987), Geological map of the Tehran quadrangle, scale 1:250,000, Geol. Surv. of Iran, Tehran.

Hassanzadeh, J. (1993), Metallogenic and tectonomagmatic events in the SE sector of the Cenozoic active continental margin of central Iran (Shahr e Babak area, Kerman Province), Ph.D. thesis, 204 pp., Univ. of Calif., Los Angeles.

Hassanzadeh, J., and M. Fakhari (1997), Oligo-Miocene marine environments of central Iran: Intra- and back-arc extensions, in *59th European Association of Geoscientists and Engineers Conference, Geneva, Switzerland*, vol. 2, edited by Petroleum Division, European Association of Geoscientists and Engineers, p. D014, Zeist, Netherlands.

Hassanzadeh, J., G. J. Axen, B. Guest, D. F. Stockli, and A. M. Ghazi (2004), The Alborz and NW Urumieh-Dokhtar magmatic belts, Iran: Rifted parts of a single ancestral arc, *Geol. Soc. Am. Abstr. Programs*, *36*(5), 434.

Hassanzadeh, J., D. F. Stockli, B. K. Horton, G. J. Axen, L. D. Stockli, M. Grove, A. K. Schmitt, and J. D. Walker (2008), U-Pb zircon geochronology of late Neoproterozoic-Early Cambrian granitoids in Iran: Implications for paleogeography, magmatism, and exhumation history of Iranian basement, *Tectonophysics*, *451*, 71–96, doi:10.1016/j.tecto.2007.11.062.

Hassanzadeh, J., B. Wernicke, and A. M. Ghazi (2009), Timing of Arabia-Eurasia collision in Iran constrained by post-collisional magmatism, *Geol. Soc. Am. Abstr. Programs*, *41*(7), 407.

Hickey, R. L., F. A. Frey, D. C. Gerlach, and L. Lopez-Escobar (1986), Multiple sources for basaltic arc rocks from the southern volcanic zone of the Andes (34°–41°S): Trace element and isotopic evidence for contributions from subducted oceanic crust, mantle, and continental crust, *J. Geophys. Res.*, *91*, 5963–5983, doi:10.1029/JB091iB06p05963.

Hollister, L. S., and C. L. Andronicos (2006), Formation of new continental crust in western British Columbia during transpression and transtension, *Earth Planet. Sci. Lett.*, *249*, 29–38, doi:10.1016/j.epsl.2006.06.042.

Horton, B. K., J. Hassanzadeh, D. F. Stockli, G. J. Axen, R. J. Gillis, B. Guest, A. Amini, M. D. Fakhari, S. M. Zamanzadeh, and M. Grove (2008), Detrital zircon provenance of Neoproterozoic to Cenozoic deposits in Iran: Implications for chronostratigraphy and collisional tectonics, *Tectonophysics*, *451*, 97–122, doi:10.1016/j.tecto.2007.11.063.

Huang, F., and C. C. Lundstrom (2007), ^{231}Pa excesses in arc volcanic rocks: Constraint on melting rates at convergent margins, *Geology*, *35*, 1007–1010, doi:10.1130/G23822A.1.

Humphreys, E. D. (1995), Post-Laramide removal of the Farallon slab, western United States, *Geology*, *23*, 987–990, doi:10.1130/0091-7613(1995)023<0987:PLROTF>2.3.CO;2.

Humphreys, E., E. Hessler, K. Dueker, G. L. Farmer, E. Erslev, and T. Atwater (2003), How Laramide-age hydration of North American lithosphere by the Farallon slab controlled subsequent activity in the

western United States, *Int. Geol. Rev.*, *45*, 575–595, doi:10.2747/0020-6814.45.7.575.

Jahangiri, A. (2007), Post-collisional Miocene adakitic volcanism in NW Iran: Geochemical and geodynamic implications, *J. Asian Earth Sci.*, *30*, 433–447, doi:10.1016/j.jseaes.2006.11.008.

Jordan, T. E., and R. W. Allmendinger (1986), The Sierras Pampeanas of Argentina: A modern analogue of Rocky Mountain foreland deformation, *Am. J. Sci.*, *286*, 737–764, doi:10.2475/ajs.286.10.737.

Jung, D., M. O. C. Kürsten, and M. Tarkian (1974), Post-Mesozoic volcanism in Iran and its relation to the subduction of the Afro-Arabian under the Eurasian plate, in *Afar Between Continental and Oceanic Rifting*, *Commiss. Geodyn. Sci. Rep.*, vol. 16, edited by A. Pilger and A. Rösler, pp. 175–181, Scheizerbart, Stuttgart, Germany.

Jung, D., J. Keller, R. Khorasani, C. Marcks, A. Baumann, and P. Horn (1984), Petrology of the Tertiary magmatic activity in the northern Lut area, east Iran, *Neues Jahrb. Geol. Palaeontol. Abh.*, *160*, 417–467.

Kargaran, F., F. Neubauer, J. Genser, and A. Houshmandzadeh (2006), The Eocene Chapedony metamorphic core complex in central Iran: Preliminary structural results, *Geophys. Res. Abstr.*, *8*, abstract 05008.

Karlsson, H. R., and R. N. Clayton (1991), Analcime phenocrysts in igneous rocks: Primary or secondary?, *Am. Mineral.*, *76*, 189–199.

Kay, R. W., and S. M. Kay (1993), Delamination and delamination magmatism, *Tectonophysics*, *219*, 177–189, doi:10.1016/0040-1951(93)90295-U.

Kay, S. M., E. Godoy, and A. Kurtz (2005), Episodic arc migration, crustal thickening, subduction erosion, and magmatism in the south-central Andes, *Geol. Soc. Am. Bull.*, *117*, 67–88, doi:10.1130/B25431.1.

Kazmin, V. G., I. M. Sbortshikov, L.-E. Ricou, L. P. Zonenshain, J. Boulin, and A. L. Knipper (1986), Volcanic belts as markers of the Mesozoic-Cenozoic active margin of Eurasia, *Tectonophysics*, *123*, 123–152, doi:10.1016/0040-1951(86)90195-2.

Lange, R. A., and I. S. E. Carmichael (1991), A potassic volcanic front in western Mexico: The lamprophyric and related lavas of San Sebastian, *Geol. Soc. Am. Bull.*, *103*, 928–940, doi:10.1130/0016-7606(1991)103<0928:APVFIW>2.3.CO;2.

Lawton, T. F., and N. J. McMillan (1999), Arc abandonment as a cause for passive continental rifting: Comparison of the Jurassic Mexican Borderland rift and the Cenozoic Rio Grande rift, *Geology*, *27*, 779–782, doi:10.1130/0091-7613(1999)027<0779:AAAACF>2.3.CO;2.

Luhr, J. F., and T. K. Kyser (1989), Primary igneous analcime: The Colima minettes, *Am. Mineral.*, *74*, 216–223.

Macdonald, G. A., and T. Katsura (1964), Chemical composition of Hawaiian lavas, *J. Petrol.*, *5*, 82–133.

Márquez, A., R. Oyarzun, M. Doblas, and S. P. Verma (1999), Alkalic (ocean-island basalt type) and calc-alkalic volcanism in the Mexican volcanic belt: A case for plume-related magmatism and propagating rifting at an active margin?, *Geology*, *27*, 51–54, doi:10.1130/0091-7613(1999)027<0051:AOIBTA>2.3.CO;2.

McCulloch, M. T., and J. A. Gamble (1991), Geochemical and geodynamical constraints on subduction zone magmatism, *Earth Planet. Sci. Lett.*, *102*, 358–374, doi:10.1016/0012-821X(91)90029-H.

McQuarrie, N., J. M. Stock, C. Verdel, and B. P. Wernicke (2003), Cenozoic evolution of Neotethys and implications for the causes of plate motions, *Geophys. Res. Lett.*, *30*(20), 2036, doi:10.1029/2003GL017992.

Moritz, R., F. Ghazban, and B. S. Singer (2006), Eocene gold ore formation at Muteh, Sanandaj-Sirjan tectonic zone, western Iran: A result of late-stage extension and exhumation of metamorphic basement rocks within the Zagros orogen, *Econ. Geol.*, *101*, 1497–1524, doi:10.2113/gsecongeo.101.8.1497.

Morley, C. K., B. Kongwung, A. A. Julapour, M. Abdolghafourian, M. Hajian, D. Waples, J. Warren, H. Otterdoom, K. Srisuriyon, and H. Kazeni (2009), Structural development of a major late Cenozoic basin and transpressional belt in central Iran: The Central Basin in the Qom-Saveh area, *Geosphere*, *5*, 325–362, doi:10.1130/GES00223.1.

Morrison, G. W. (1980), Characteristics and tectonic setting of the shoshonite rock association, *Lithos*, *13*, 97–108, doi:10.1016/0024-4937(80)90067-5.

Noble, D. C. (1972), Some observations on the Cenozoic volcano-tectonic evolution of the Great Basin, western United States, *Earth Planet. Sci. Lett.*, *17*, 142–150, doi:10.1016/0012-821X(72)90269-5.

Omrani, J., P. Agard, H. Whitechurch, M. Benoit, G. Prouteau, and L. Jolivet (2008), Arc magmatism and subduction history beneath the Zagros Mountains, Iran: A new report of adakites and geodynamic consequences, *Lithos*, *106*, 380–398, doi:10.1016/j.lithos.2008.09.008.

Pazirandeh, M. (1973), Distribution of volcanic rocks in Iran and a preliminary discussion of their relationship to tectonics, *Bull. Volcanol.*, *37*, 573–585, doi:10.1007/BF02596892.

Pearce, J. A., and J. R. Cann (1973), Tectonic setting of basic volcanic-rocks determined using trace-element analyses, *Earth Planet. Sci. Lett.*, *19*, 290–300, doi:10.1016/0012-821X(73)90129-5.

Pearce, J. A., and I. J. Parkinson (1993), Trace element models for mantle melting: Application to volcanic arc petrogenesis, in *Magmatic Processes and Plate Tectonics*, edited by H. M. Prichard et al., *Geol. Soc. Spec. Publ.*, *76*, 373–403.

Plank, T., and C. H. Langmuir (1988), An evaluation of the global variations in the major element chemistry of arc basalts, *Earth Planet. Sci. Lett.*, *90*, 349–370, doi:10.1016/0012-821X(88)90135-5.

Plank, T., and C. H. Langmuir (1993), Tracing trace elements from sediment input to volcanic output at subduction zones, *Nature*, *362*, 739–742.

Pollastro, R. M., F. M. Persits, and D. W. Steinshouer (Comps.) (1999), Map showing geology, oil and gas fields, and geologic provinces of Iran [CD-ROM], *U.S. Geol. Surv. Open File Rep.*, 97-470-G.

Prelević, D., S. F. Foley, V. Cvetković, and R. L. Romer (2004), The analcime problem and its impact on the geochemistry of ultrapotassic rocks from Serbia, *Mineral. Mag.*, *68*, 633–648, doi:10.1180/0026461046840209.

Ramezani, J., and R. D. Tucker (2003), The Saghand region, central Iran: U-Pb geochronology, petrogenesis and implications for Gondwana tectonics, *Am. J. Sci.*, *303*, 622–665, doi:10.2475/ajs.303.7.622.

Reuter, M., W. E. Piller, M. Harzhauser, O. Mandic, B. Berning, F. Rögl, A. Kroh, M.-P. Aubry, U. Wielandt-Schuster, and A. Hamedani (2009), The Oligo-/Miocene Qom Formation (Iran): Evidence for an early Burdigalian restriction of the Tethyan Seaway and closure of its Iranian gateways, *Int. J. Earth Sci.*, *98*, 627–650, doi:10.1007/s00531-007-0269-9.

Rhodes, J. M. (1996), Geochemical stratigraphy of lava flows sampled by the Hawaii Scientific Drilling Project, *J. Geophys. Res.*, *101*, 11,729–11,746, doi:10.1029/95JB03704.

Sengör, A. M. C., A. Cin, D. B. Rowley, and S.-Y. Nie (1993), Space-time patterns of magmatism along the Tethysides: A preliminary study, *J. Geol.*, *101*, 51–84, doi:10.1086/648196.

Shahabpour, J. (2007), Island-arc affinity of the central Iranian volcanic belt, *J. Asian Earth Sci.*, *30*, 652–665, doi:10.1016/j.jseaes.2007.02.004.

Sheth, H. C., I. S. Torres-Alvarado, and S. P. Verma (2002), What is the "calc-alkaline rock series"?, *Int. Geol. Rev.*, *44*, 686–701, doi:10.2747/0020-6814.44.8.686.

Sisson, T. W., and S. Bronto (1998), Evidence for pressure-release melting beneath magmatic arcs from basalt at Galunggung, Indonesia, *Nature*, *391*, 883–886, doi:10.1038/36087.

Spies, O., G. Lensch, and A. Mihm (1984), Petrology and geochemistry of the post-ophiolitic Tertiary volcanics between Sabzevar and Quchan, NE Iran, *Neues Jahrb. Geol. Palaeontol. Abh.*, *168*, 389–408.

Stampfli, G. M., and G. D. Borel (2002), A plate tectonic model for the Paleozoic and Mesozoic constrained by dynamic plate boundaries and restored synthetic oceanic isochrons, *Earth Planet. Sci. Lett.*, *196*, 17–33, doi:10.1016/S0012-821X(01)00588-X.

Stöcklin, J. (1968), Structural history and tectonics of Iran: A review, *Am. Assoc. Pet. Geol. Bull.*, *52*, 1229–1258.

Stöcklin, J., and A. Setudehnia (1977), *Stratigraphic Lexicon of Iran*, 2nd ed., *Rep. 18*, 376 pp., Geol. Surv. of Iran, Tehran.

Sun, S. S., and W. F. McDonough (1989), Chemical and isotopic systematics of oceanic basalts: Implications for mantle composition and processes, in *Magmatism in the Oceanic Basins*, edited by A. D. Saunders and M. J. Norry, *Geol. Soc. Spec. Publ.*, *42*, 313–345.

Takin, M. (1972), Iranian geology and continental drift in the Middle East, *Nature*, *235*, 147–150, doi:10.1038/235147a0.

Tatsumi, Y., D. L. Hamilton, and R. W. Nesbitt (1986), Chemical characteristics of fluid phase released from a subducted lithosphere and origin of arc magmas: Evidence from high-pressure experiments and natural rocks, *J. Volcanol. Geotherm. Res.*, *29*, 293–309, doi:10.1016/0377-0273(86)90049-1.

Taylor, S. R., and S. M. McLennan (1985), *The Continental Crust: Its Composition and Evolution—An Examination of the Geochemical Record Preserved in Sedimentary Rocks*, 312 pp., Blackwell Sci., Oxford, U. K.

Tillman, J. E., A. Poosti, S. Rossello, and A. Eckert (1981), Structural evolution of Sanandaj-Sirjan Ranges near Esfahan, Iran, *AAPG Bull.*, *65*, 674–687.

Van Buer, N. J., and E. L. Miller (2010), Sahwave Batholith, NW Nevada: Cretaceous arc flare-up in a basinal terrane, *Lithosphere*, *2*, 423–446, doi:10.1130/L105.1.

Verdel, C., B. P. Wernicke, J. Ramezani, J. Hassanzadeh, P. R. Renne, and T. L. Spell (2007), Geology and thermochronology of Tertiary Cordilleran-style metamorphic core complexes in the Saghand region of central Iran, *Geol. Soc. Am. Bull.*, *119*, 961–977, doi:10.1130/B26102.1.

Verma, S. P. (2002), Absence of Cocos plate subduction-related basic volcanism in southern Mexico: A unique case on Earth?, *Geology*, *30*, 1095–1098, doi:10.1130/0091-7613(2002)030<1095:AOCPSR>2.0.CO;2.

Vernant, P., et al. (2004), Present-day crustal deformation and plate kinematics in the Middle East constrained by GPS measurements in Iran and northern Oman, *Geophys. J. Int.*, *157*, 381–398, doi:10.1111/j.1365-246X.2004.02222.x.

Vincent, S. J., M. B. Allen, A. D. Ismail-Zadeh, R. Flecker, K. A. Foland, and M. D. Simmons (2005), Insights from the Talysh of Azerbaijan into the Paleogene evolution of the South Caspian region, *Geol. Soc. Am. Bull.*, *117*, 1513–1533, doi:10.1130/B25690.1.

Wallace, P. J., and I. S. E. Carmichael (1999), Quaternary volcanism near the Valley of Mexico: Implications for subduction zone magmatism and the effects of crustal thickness variations on primitive magma compositions, *Contrib. Mineral. Petrol.*, *135*, 291–314, doi:10.1007/s004100050513.

Wallace, P., I. S. E. Carmichael, K. Righter, and T. A. Becker (1992), Volcanism and tectonism in western Mexico: A contrast of style and substance, *Geology*, *20*, 625–628, doi:10.1130/0091-7613(1992)020<0625:VATIWM>2.3.CO;2.

Wernicke, B. (1992), Cenozoic extensional tectonics of the U.S. Cordillera, in *The Cordilleran Orogen: Conterminous U.S.*, vol. G-3, edited by B. C. Burchfiel et al., pp. 553–581, Geol. Soc. of Am., Geol. of North Am., Boulder, Colo.

Wilmsen, M., F. T. Fürsich, K. Seyed-Emami, M. R. Majidifard, and J. Taheri (2009), The Cimmerian Orogeny in northern Iran: Tectono-stratigraphic evidence from the foreland, *Terra Nova*, *21*, 211–218, doi:10.1111/j.1365-3121.2009.00876.x.

Woodhead, J. D., S. E. Eggins, and J. G. Gamble (1993), High field strength and transition element systematics in island arc and back-arc basin basalts: Evidence for multi-phase extraction and a depleted mantle wedge, *Earth Planet. Sci. Lett.*, *114*, 491–504, doi:10.1016/0012-821X(93)90078-N.

B. Guest, Department of Geoscience, University of Calgary, Calgary, AB T2N 1N4, Canada.

J. Hassanzadeh and B. P. Wernicke, Division of Geological and Planetary Sciences, California Institute of Technology, Pasadena, CA 91125, USA.

C. Verdel, Department of Geology, University of Kansas, Lawrence, KS 66045, USA. (cverdel@ku.edu)